TÉCNICO LISBOA

Effects of potassium and calcium on the combustion behaviour of biomass

André Vasconcelos de Carvalho

Thesis to obtain the Master of Science Degree in

Mechanical Engineering

Supervisors: Prof. Mário Manuel Gonçalves da Costa,
Prof. Miriam Estefânia Rodrigues Fernandes Rabaçal

Examination Committee

Chairperson: Prof. Edgar Caetano Fernandes
Supervisor: Prof. Miriam Estefânia Rodrigues Fernandes Rabaçal
Member of the Committee: Prof. Luís António da Cruz Tarelho

July 2017

ACKNOWLEDGEMENTS

I would like to thank my supervisors, Prof. Mário Costa and Prof. Miriam Rabaçal, for the support, guidance, availability and teachings given during the elaboration of this master's thesis.

I also want to thank María Abián for her friendship and for the help given during the experimental work and the dissertation in general.

I wish to thank Manuel Pratas, my colleagues and friends from the laboratory, for the good times spent and support given during this work.

I would like to thank all the people I met during the development of this dissertation, and who somehow contributed to its elaboration.

Finally, I thank my family, my friends and Cláudia for their support, patience and understanding throughout my academic years.

RESUMO

O principal objetivo deste trabalho é avaliar os efeitos dos elementos potássio (K) e cálcio (Ca) na combustão de biomassa a baixas e altas taxas de aquecimento. A biomassa utilizada foi o bagaço de uva, peneirado na gama de granulometrias 200-250 μm. Usando processos de desmineralização e impregnação, foram obtidas 12 amostras diferentes: original, desmineralizada e impregnadas com 0,1, 0,5, 0,82, 3 e 6% em massa de K e 0,1, 0,5, 1,08, 3 e 6% em massa de Ca. Inicialmente, para identificar o papel individual de K e Ca, foram realizados ensaios de pirólise e combustão às amostras de biomassa num analisador termogravimétrico (TGA). Em geral, o processo de combustão foi promovido com aumento da concentração de K, enquanto o Ca não influenciou significativamente este processo. Os ensaios a altas taxas de aquecimento foram realizados num queimador de chama plana McKenna a duas condições de operação distintas. Uma câmara de alta velocidade foi usada para captar as fases iniciais do processo de combustão, em particular os eventos de ignição e combustão de voláteis. Os resultados obtidos mostraram que a impregnação de K levou a uma diminuição do tempo de atraso à ignição, enquanto a impregnação de Ca não teve um impacto significativo. Ambos os pré-tratamentos de impregnação diminuíram o tempo de combustão dos voláteis com o aumento das concentrações de K ou Ca. Finalmente, as impregnações com K e Ca tiveram um impacto mais significativo no tempo de combustão dos voláteis do que no tempo de atraso à ignição.

Keywords:

Potássio, cálcio, análise termogravimétrica, partículas isoladas, tempo de atraso à ignição, tempo de combustão de voláteis.

ABSTRACT

The main objective of this work is to evaluate the effects of potassium (K) and calcium (Ca) on the combustion behaviour of biomass at low and high heating rates. The biomass used was grape pomace, sieved in the size range of 200-250 µm. With the pre-treatments of demineralization and impregnation, a total of 12 different samples were obtained: raw, demineralized and impregnated grape pomace with 0.1, 0.5, 0.82, 3 and 6 wt.% of K, and 0.1, 0.5, 1.08, 3 and 6 wt.% of Ca. Firstly, to identify the individual role of K and Ca, the biomass samples were pyrolyzed in a N_2 atmosphere and oxidized in air using a thermogravimetric analyser (TGA). In general, the combustion process was promoted with increasing K concentration, whereas Ca did not significantly influence this process. The high heating rate tests were performed in a McKenna burner at two different operating conditions. A CMOS high-speed camera was used to record the ignition and the volatiles combustion events. The results obtained showed that K impregnation led to a decrease in the ignition delay time as the concentration of K increased, while Ca impregnation did not have a significant impact on the ignition delay time. Both impregnation pre-treatments decreased the volatiles combustion time as the concentration of K or Ca increased. Finally, the impregnation with K and Ca had a more significant impact on the volatiles combustion time than on the ignition delay time.

Keywords:

Potassium, calcium, thermogravimetric analysis, single particle, ignition delay time, volatile combustion time

PUBLICATIONS ORIGINATED FROM THIS THESIS

Carvalho A, Rabaçal M, Costa M, Abián M, Alzueta MU. Effects of potassium and calcium on the early stages of combustion of single biomass particles. Submitted to Fuel, 2017.

Abián M, Alzueta MU, Carvalho A, Rabaçal M, Costa M. On the role of potassium and calcium on the combustion characteristics of biomass obtained from thermogravimetric experiments. Submitted to Fuel, 2017.

Abián M, Alzueta MU, Carvalho A, Rabaçal M, Costa M. On the role of Calcium and Potassium on the Combustion Characteristics of Biomass: From Particle Ignition to Char Oxidation. Joint Meeting of the Portuguese & Scandinavian Nordic Sections of the Combustion Institute 17-18 November 2016, Lisbon, Portugal.

Abián M, Alzueta MU, Carvalho A, Rabaçal M, Costa M. Impact of Calcium and Potassium on Single Particle Ignition Behaviour of Biomass Fuels. SMARTCATs 2nd General Meeting 14-16 November 2016, Lisbon, Portugal.

TABLE OF CONTENTS

LIST OF FIGURES

LIST OF TABLES

NOMENCLATURE

Symbols

Bi	Biot number
m	Mass
m_0	Initial mass
$\dot{Q}_{cat}$	Heat transfer associated with the induced catalytic reactions
$\dot{Q}_{cond}$	Heat transfer by conduction
$\dot{Q}_{conv}$	Heat transfer by convection
$\dot{Q}_{rad}$	Heat transfer by radiation
t_{ig}	Ignition delay time
t_{vol}	Volatile combustion time
X	Biomass conversion

Greek Letters

λ	Excess air coefficient

Acronyms

AAEM	Alkali and alkaline earth metals
CMOS	Complementary metal oxide semiconductor
DTG	Differential thermogravimetric
DTF	Drop tube furnace
EDS	Energy-dispersive X-ray spectroscopy
EFR	Entrained flow reactor
FC	Fixed carbon
FPS	Frames per second
ICCD	Intensified charge coupled device
MToe	Million tones of oil equivalent
PT	Peak temperature
SEM	Scanning electron microscope
TGA	Thermogravimetric analysis
VM	Volatile matter
wt	Weight

1. INTRODUCTION

1.1. MOTIVATION

Energy sustainability is one of the main concerns of today's society as energy demand and consumption have been increasing over the years due to population growth and income of the various countries mostly derived from improvements in productivity. Due to this, the production of energy in its several forms needs to follow the consumption needs, always taking into account the environmental, economic and social impact of the use of renewable and non-renewable energy sources. The global primary energy consumption (in Mtoe) has significantly increased over the last decades with an accountable value of 53% of change from 1995 to 2015 [1]. Despite this considerable growth, the rate at which the global primary energy consumption increases has been decreasing in the past years, being the growth only 1.1% for the year of 2014 and 1.0% for the year of 2015 [2]. There is an apparent stagnation that may be due to advances in the technology available and improvements in energy efficiency, it is still expected that global primary energy consumption increases 31% from 2015 to 2035 [1].

Current energy needs still depend significantly on fossil fuel utilization, because the growth of energy production derived from renewable sources is still not sufficient to keep up with the global primary energy consumption growth. Coal is still one of the main non-renewable sources and it is manly used in power plants. For this fossil fuel, it has been verified a decrease in both production (4%) and consumption (1.8%) in the year of 2015, yet coal will continue to be a major non-renewable source of energy not only because of its high levels of production and consumption but due to its abundance in nature [2]. Coal presents the highest reserve-to-production ratio compared with other fossil fuels in which the reserve stock in 2015 would be enough to match the coal production of 2015 for another 114 years [2].

There are some issues that arise from burning coal and other fossil fuels, with the emission of pollutants being one of the main problems. Pollutant emission is a subject of great interest for society due to the environmental and health problems that arise from it. Currently its limitation and control is one of the main objectives inherent to the application of combustion processes. The main pollutant species emitted to the atmosphere from burning fossil fuels are CO_2, CO, NO_x, SO_x, PAH and particles. Carbon dioxide is the main product resulting from the burning of fossil fuels and despite being essential for plants due to the photosynthesis phenomenon, its emission into the atmosphere contributes to the greenhouse effect and consequently to global warming. The energy sector is the main contributor for the anthropogenic emissions of greenhouse gases, with CO_2 being the product with the greatest contribution. CO_2 emissions due to the energy consumption of burning fossil fuels increased by 0.1% in 2015 [2]. It is expected that CO_2 emissions will increase 13% by the year of 2035 [1].

To minimize the problem of pollutant emissions, there has been a growing interest worldwide in changing the fuel mix and give higher emphasis to biofuels in the energy sector, due not only to environmental reasons but also to economic and social reasons by reducing the dependence on imported fossil fuels and increasing employability [3,4]. These biofuels can be used individually or

together with fossil fuels in co-firing systems. Biomass is an important renewable energy source as a consequence of its rapid growth, collection and production compared with fossil fuels, and can be used in power plants individually or together with coal in co-firing systems. An important advantage of biomass is its neutrality regarding the CO_2 emission point of view. This neutrality results from the equality obtained between the consumption of CO_2 during photosynthesis and its release during combustion. Due to its great abundance and renewable nature, biomass as solid biofuel can play a key role in global energy production in which the residual biomass from agricultural and industrial activity can have a positive social and economic impact on its local use [5].

However, despite the advantages presented, there are some issues and challenges regarding the energy use of biomass, namely in its preparation and in the combustion process [6]. The difficulties of biomass application in thermochemical conversion technologies arise from the fact that biomass is has high heterogeneity, presents a low calorific value, presents flame instabilities due to the high reactivity of the volatile matter, which is present in large quantities, presents high moisture content that can cause ignition and combustion problems, and has issues concerning the ash content with the formation of slag and deposits [6–8]. The ash content differs greatly for each type of biomass depending on its origin and biological diversity; it is generally formed by Si, Cl, S, alkali metals (Na, K), alkaline earth metals (Mg, Ca) and heavy metals. Most of these elements are bounded to the organic compounds present in the biomass, which are decomposed during the combustion, thus releasing ash-forming elements [9–11]. The ash formation is one of the main problems to handle and consider in thermal conversion technologies in thermoelectric power plants because they are responsible for problems such as particle emissions, slagging, deposition, ash fusion, agglomeration and corrosion. For example, biomass with higher contents of Cl and alkali metals (K and Na) may increase rapidly the slag and deposit formation on the heating surfaces, which may introduce corrosion problems underneath the deposits thereafter, if the accumulated ash has a high content of Cl [6]. These problems reduce the thermal conversion efficiency, reduce the life-time and increase equipment operation and maintenance costs, which can lead to prolonged and unplanned shutdowns of the combustion units [6,12–15].

The alkali and alkaline earth metals of biomass are elements that play a fundamental role not only in the ash formation. They also have a role in the catalytic action during combustion [16]. Alkali and alkaline earth metals, although present in biomass at low concentrations compared to the main organic constituents, can influence the ignition and combustion process as a whole, and the formation and emission of pollutants. Generally, these elements represent 1% of the weight of lignocellulosic biomass residues, but they can reach up to 15% in some forest and herbaceous residues [17]. Many studies focused on studying the catalytic effect of elements like potassium during pyrolysis and char combustion at low temperatures and heating rates [13,18–20]. These studies were mostly performed in reactors where the particles were in a fixed position or in thermogravimetric analyzers. There is a gap in the literature regarding the catalytic behaviour of alkali and alkaline earth metals under conditions typical of those encountered in industrial pulverized systems. In this context, the present work focuses on the catalytic effect of alkali and alkaline earth metals, particularly potassium and calcium, on the combustion behaviour of grape pomace, which is a residue formed during wine production with high potential to be

used as fuel for local energy production, and their impact on the ignition of pulverized single biomass particles.

1.2. THEORETICAL FOUNDATIONS

1.2.1 BIOMASS CHARACTERIZATION

Biomass can be defined as any solid biodegradable organic material that can be burned and used as fuel [6], and can be classified according to its source and origin into the following groups: (1) wood (oak, pine, beech, etc.) and woody biomass (branches, bushes, leaves, etc.), (2) herbaceous and agricultural biomass (grasses, straws, husks, shells, etc.), (3) aquatic biomass (microalgae, seaweed, sweet-water weeds, etc.), (4) animal and human biomass wastes (bones, chicken litter, etc.) (5) contaminated biomass and industrial biomass wastes (municipal solid waste, sewage sludge, etc.), (6) biomass mixtures [11]. Due to its origin and biological diversity, biomass is quite heterogeneous, presenting variable contents of the organic and inorganic compounds that constitute it. Generally, the main elements that form the organic part of the biomass are Carbon (C), Oxygen (O), Hydrogen (H) and Nitrogen (N) and the inorganic part, usually known as ash-forming elements, Silicon (Si), Calcium (Ca), Magnesium (Mg), Potassium (K), Sodium (Na), Iron (Fe), Phosphorus (P), Chlorine (Cl), Sulfur (S), Aluminium (Al), and residual elements like Titanium (Ti) and Manganese (Mn). These inorganic elements are not present in the biomass individually, being commonly bound to the organic matter occurring in the form of oxides and hydroxides, carbonates, sulphates, chlorides, phosphates, nitrates and silicates and can be determined quantitatively by ultimate and ash analysis [11,21,22].

The organic matter present in the biomass (lignocellulose) is structured in cellulose, hemicellulose and lignin. The composition of these constituents in weight percentage in dry basis varies greatly depending on the species of biomass considered, although generally it has between 40-60% cellulose, 20-40% hemicellulose and 15-25% lignin [3,23,24]. Hemicellulose consists of a mixture of heterogeneously branched polysaccharides composed of sugars such as xylose and other five carbon monosaccharides. It has an amorphous and irregular structure with branches that are easily degraded with the release of volatiles [23]. Cellulose is a strong non-branched structure consisting of a long glucose polymer and a high thermal stability [23]. Lignin is an amorphous structure composed of aromatic rings with several branches whose proportion varies according to the origin of the biomass being the chemical bonds degraded for a wide range of temperatures (373-1173 K) [3,22,23].

Biomass can be characterized by the proximate analysis, listing its moisture content, volatile matter, fixed carbon and ash content. The moisture content of biomass is a relevant factor to be taken into account in thermal conversion technologies because these require the moisture content to be typically less than 50% to be efficient and energetically feasible [3]. This parameter differs from biomass to biomass and depends on factors such as the climate conditions and techniques used during biomass harvest and the consequent time and storage circumstances [25,26]. The volatile matter consists of material released in the gas-phase as a consequence of heating and burning, while the fixed carbon is the solid combustible mass that remains after the volatile matter has been released [3]. The ratio of

volatile matter to fixed carbon (VM/FC) of biomass is typically greater than 4 while for coal it is typically less than 1. This may indicate that biomass presents a characteristic combustion in the gas-phase with the oxidation of the volatile species, making it a fuel with high reactivity facilitating, therefore, its thermochemical conversion [3,27,28]. The ash corresponds to the solid residue that results from the combustion of the solid fuel. The inorganic matter and ash-forming elements present in the biomass are typically between values of 0.1-8.4% for wood and woody type biomass and between 0.8-18.6% for herbaceous and agricultural biomass. The high range of ash content observed for the latter type of biomass is due to the high variability of sources and biological heterogeneous diversity of biomass residues present in this group (grasses, straws, husks, shells, residues, etc.) [11]. The ash content of biomass varies greatly depending on its source and part considered. It also depends on the nutrients, soil quality, fertilizers and weather conditions during its growth, formation and harvest [27,29].

1.2.2 FUNDAMENTS OF IGNITION AND COMBUSTION OF BIOMASS

The combustion process of biomass particles can be divided into four main phases: (1) heating and drying phase, (2) devolatilization and ignition, (3) volatiles combustion and (4) char oxidation [30]. Due to the high heating rates verified in pulverized combustion systems, the last two stages can occur indistinctly, with a certain degree of overlap [31]. Figure 1 shows a schematic of the combustion of a biomass particle. It's important to note that fragmentation, despite not being represented, is a phenomenon that can occur during biomass combustion.

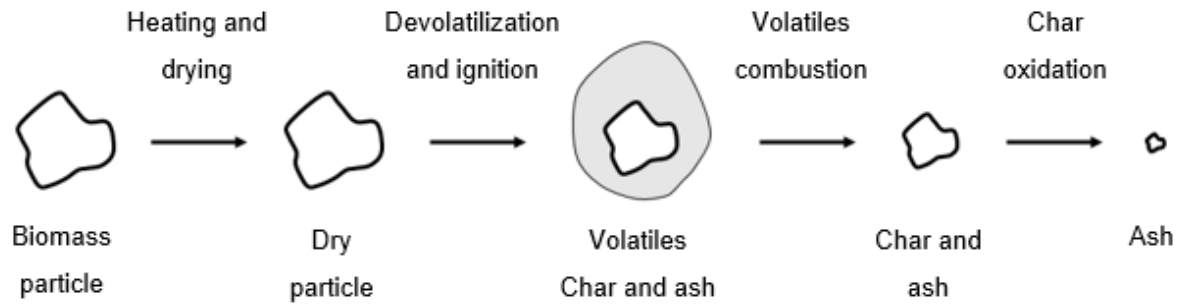

Figure 1. Schematic of the combustion process of a biomass particle (adapted from [32]).

The combustion process of a biomass particle starts with the heating and drying phase, which is an endothermic process controlled by heat transfer that starts at 105 C° [30]. It consists on the release of moisture from the particle into the gas-phase. The moisture content determines the energy required for self-sustained combustion with the latent heat of vaporization, which turns out to be impractical for moisture contents above 50% [3]. The next phase is the devolatilization that is the process of releasing the volatile matter present in the solid fuel during its continuous heating, being directly related to the decomposition of the organic structures of biomass (hemicellulose, cellulose and lignin) [33,34]. The

main released species are H_2, NH_3, O_2, CO, CO_2, H_2O, CH_4, CH_3OH, HCOOH and tars [8]. There are several parameters that influence the devolatilization of biomass particles such as the shape, the size, the initial mass of the biomass particles, the heating rate and the temperature [33,35,36]. At the beginning of devolatilization ignition occurs. Ignition of a mixture of reagents can be defined as a non-stationary process where radicals form, releasing heat and rapidly increasing temperature, giving rise to a self-sustained combustion phenomenon [30]. This ignition process is relevant and has been widely studied to understand the combustion process of solid fuels. Ignition of biomass particles can occur in two distinct ways, commonly known as the ignition modes: gas-phase (homogeneous) ignition and surface (heterogeneous) ignition. The ignition mode depends on factors such as heating rate, temperature, oxygen concentration, particle size, shape and composition [37]. Ignition generally occurs in the gas-phase during the devolatilization. The volatiles burn in a cloud-shape volatile flame around the particle until all the volatile matter released has been consumed. When the oxygen is able to diffuse to the surface of the particle, which may occur with or even before the extinction of the volatile flame around the particle, heterogeneous char oxidation occurs. The surface ignition occurs when the oxygen is able to diffuse rapidly to the particle surface, when a significant amount of volatile matter hasn't been released yet, making the volatiles and char burning simultaneously at the particle surface. The char is a residue essentially composed by carbon and ashes and small amounts of hydrogen, oxygen, nitrogen, and sulphur and has an irregular porous structure in case of biomass. Char oxidation is a much slower process than devolatilization. Its reactivity depends on its morphological structure, which in turn is influenced by the particle size, volatile release and quantity and composition of the inorganic matter present [38,39]. The char residue presents a porous structure as a result of the volatile matter release, which is influenced by the heating rate. The greater the char porosity, the greater its accessible surface area for the gas mixture, increasing its reactivity [40]. It is important to note that during the combustion process, the inorganic material may catalyze the reactions, particularly during the devolatilization and char oxidation stages [16].

1.3. PREVIOUS STUDIES

1.3.1 BIOMASS DEMINERALIZATION AND IMPREGNATION

In order to study the influence of the mineral content in thermochemical conversion processes using biomass, demineralization/leaching procedures using water or diluted acid solutions as leaching agents are generally applied [17,19,24,41–46]. This pre-treatment is typically used when it is desired to remove most of the inorganic elements with possible catalytic effects on biomass thermal degradation, followed by an impregnation procedure to place a certain element in the biomass in order to evaluate its catalytic activity. Thus, demineralization/leaching pre-treatments usually involve the following four steps: (i) preparation of the sample and the aqueous solution with the demineralization agent, (ii) mixing and stirring the sample in the aqueous solution, (iii) washing and filtering, and (iv) drying the sample. The choice of the acidic aqueous solution to be used in the removal of the minerals present in the biomass samples is an important factor to be considered. In this context, Eom et al. [24] studied the

influence of four different leaching agents (distilled water, tap water, HCl and HF) in order to investigate the effect of the demineralization process in the pyrolysis behaviour of biomass. The authors verified that distilled water does not remove the inorganic matter efficiently and tap water has the opposite effect to that desired by increasing the concentration of inorganic matter, particularly calcium. It was also found that HCl efficiently removes inorganic matter, but also removes some of acid-soluble hydrocarbons affecting the organic structure of biomass (hemicellulose, cellulose and lignin). And, although HF does not affect the organic structure significantly, it is not efficient in removing alkaline earth metals such as calcium and magnesium. Asadieraghi et al. [42] found that demineralization through strong diluted acid solutions is effective in removing the inorganic matter from biomass where the acid strength, according to the removal verified, follows the order: $HClO_4$ > HCl > H_2SO_4 > HNO_3 > HF. However, Jiang et al. [17] verified that the treatment with strong acid solutions, such as HCl, H_2SO_4 and HNO_3, introduces undesirable physicochemical structure changes, particularly in the organic matter structure of biomass, with sulfuric acid being the treatment that most affects this structure, dissolving hemicellulose and cellulose. Another disadvantage is that biomass may be undesirably contaminated with S, Cl or N by using strong acids with these elements. Jiang et al. [17] also studied the effect of inorganics removal using weak acid solutions (CH_3COOH, H_3PO_4) revealing that these acid solutions do not have a significant impact on the physicochemical structure of biomass; however, they are less efficient in removing the inorganic matter than strong acid solutions. Additionally, the acetic acid (CH_3COOH), in contrast with strong acid solutions, hardly has adverse effect on the treated biomass since it only consists of C, O and H [47]. Mourant et al. [41] applied water and acid washing procedures with deionized water and diluted acid solution of HNO_3 to remove the main alkali and alkaline earth metal (AAEM) species from Malle wood. It was observed that deionized water could remove quite easily the elements K, Na and Mg, with the problematic element being Ca that even with increasing immersing time was not successfully removed. Acid washing with HNO_3, on the contrary, completely removed all the AAEM species. This acid washing procedure may give the idea that the physiochemical structure of biomass with emphasis on the organic structure may be strongly affected, but Perander et al. [43] applied a demineralization process using a diluted solution of HNO_3 and verified that this treatment did not introduce significant alterations in the organic structure of the biomass, namely in the component cellulose.

Following demineralization procedures, impregnation pre-treatments are typically used to place the inorganic elements of interest in the biomass samples in order to study their isolated effect on the thermochemical conversion processes. Dry mixing is another technique that can be used to do the metal addition, however, dry addition does not lead to the formation of chemical bounds between inorganic salts and the organic phase [45]. The impregnation is typically done using aqueous solutions of the element to be studied followed by stirring and drying. Several authors studied the effect of potassium on the pyrolysis behaviour of biomass by using solutions of this metal to impregnate the biomass [18,19,21,44,46,48]. Nowakowski et al. [19] studied the influence of potassium as a catalyst during pyrolysis by impregnating samples of demineralized short willow rotation coppice with a potassium acetate solution. Jensen et al. [46] studied the effects of potassium on wheat straw pyrolysis through washing the sample with a solution of KCl after leaching it with deionized water. Eom et al. [48]

investigated the effect of the elements K, Mg and Ca separately on the thermal degradation (pyrolysis) of biomass by impregnating the samples with solutions of chlorides of these elements (KCl, $CaCl_2$, $MgCl_2$). However, these compounds, similarly in the case of the demineralization treatment with some solvents, may introduce unwanted elements, in this case Cl, that can contaminate the biomass sample. Another study done by Mayer et al. [45] used a different procedure of ion-exchange to add the metals Zn and Pb to wood biomass particles after demineralization. The procedure consisted on immersing the wood samples in solutions of $Zn(NO_3)_2$ and $Pb(NO_3)_2$ followed by stirring for a longer time (100 h). Then, the samples were filtered and washed. The main difference from typical impregnation methods lied in the immersing the wood samples in deionized water for several days until equilibrium was reached and the conductivity of the water stopped increasing. This technique is intended to simulate the effect of chemically bounded minerals and to be sure that they are really chemically bounded and not only adsorbed on the surface of the biomass particles. In another work, Perander et al. [43] used $CaC_2O_4 \cdot H_2O$ (calcium oxalate monohydrate) to wet-impregnate previously acid-washed wood. In bark and forest residue biomass fuels, 70% of the total Ca is present as acid-soluble calcium oxalate minerals (CaC_2O_4) [49]. By impregnating $CaC_2O_4 \cdot H_2O$, contrary to what happens with KCl compounds, it does not introduce elements like Cl that can have adverse effects on the treated biomass, due to its composition being made of C, O and H elements.

1.3.2 POTASSIUM AND CALCIUM CHEMISTRY IN BIOMASS COMBUSTION

During combustion, the decomposition of the organic structures of biomass is accompanied by the release of its mineral constituents. Once released, the metals can be transported in the combustion gas as either solid particles or vapor species [6], depending on the given element considered. Although the mineral content depends on the type of biomass [14,15], potassium (K) is typically the main alkali and calcium (Ca) the main alkaline earth metal present in biomass [11]. Usually, K is regarded as an undesirable biomass component due to its critical role in important ash-related problems (e.g. alkali-induced slagging, silicate melt-induced slagging, ash fusion and bed agglomeration) [6]. In contrast, and despite the calcium sulfates deposits found on the cold reactor surfaces, Ca can inhibit the occurrence of silicate melt-induced slagging and bed agglomeration, due to the formation of melting calcium potassium phosphates and silicates at high temperatures [6].

Potassium is mostly present in biomass in a soluble form (e.g. in an ionic form in salts or as organically bound K ions) [6]. The potassium release from biomass is a complex subject and several pathways with mechanistic approaches have been studied and are still being studied in order to understand not only the process of its release during thermal treatments of biomass but also to “track” its behaviour as gas-phase compounds with elements like Cl and S that are responsible for problems of deposition and corrosion.

Two characteristic temperature intervals have been identified for the release of K, as alkali metal, during biomass pyrolysis [20]. Potassium associated with the organic phase is expected to be released coinciding with the onset of the pyrolysis process (453-773 K), whereas inorganic K, from the ash component of the resulting char, would be released at higher temperatures (> 773 K).

During combustion, the soluble K is mainly released into the gas-phase as K (g), KOH (g) and KCl (g) provided that Cl is available. Its release can start very early during devolatilization as the organic structure starts to decompose at low temperatures. This release is associated with the decomposition of alkaline carboxylate (573 K) and phenol-associated K (673 K) [50,51]. The decomposition of the carboxyl groups is described by the mechanism:

$$\text{Char-COOK} \leftrightarrow \text{Char} + CO_2(g) + K \quad (1)$$

where potassium is released as atomic K. At low temperatures, the atomic K can react with the phenol groups still present in the biomass through the following reaction:

$$\text{Char-}C_6H_5\text{-OH} + K \leftrightarrow \text{Char-}C_6H_5\text{-OK} + H \quad (2)$$

The thermal decomposition of the phenol groups at 673 K may lead to the release of a fraction of potassium to the gas-phase as K(g). The remaining organic-bounded K may form K_2CO_3, which is a stable compound at temperatures below 1123 K. If there is Cl in the biomass, it will be mostly present in biomass in the KCl(s) form and it was verified that for fuels with low content of Cl, most of Cl is released at 773 K through the reaction:

$$\text{Char-COOH} + KCl(s) \leftrightarrow \text{Char-COOK} + HCl(g) \quad (3)$$

However there is still a possibility for the release of KCl(s) at higher temperature ranges (973-1073 K) as it vaporizes into the gas-phase. Despite these reactions, a large fraction of potassium will remain in the particle at temperatures around 1073 K. In the temperature range of 1073-1423 K, a possible route and the most common one considered for potassium release for biomass residues with low Cl and S content is the thermal decomposition of K_2CO_3, which is enhanced by the presence of H_2O, according to [50,51]:

$$K_2CO_3\,(s) + H_2O\,(g) \leftrightarrow 2\,KOH\,(g) + CO_2\,(g) \quad (4)$$

$$K_2CO_3\,(s) \leftrightarrow K_2O\,(s) + CO_2\,(g) \quad (5)$$

$$K_2CO_3\,(s) \leftrightarrow 2K(g) + CO_2(g) + 1/2O_2(g) \quad (6)$$

At these high temperatures, if the biomass fuel has a high Si content, K may stay in the particle and form potassium silicate compounds that will probably stay in the ash.

During biomass conversion, K can also act as a catalyst for the char combustion stages of biomass [19,20,52]. Kopyscinski et al. [53] identified the following cycle for the K catalyzed gasification of char:

$$COK \rightarrow \sim K + CO \quad (7)$$

$$\sim K + C \rightarrow K\sim C \quad (8)$$

$$K\sim C + CO_2 \rightarrow COK + CO \quad (9)$$

where ~ K is a reduced K-complex.

Potassium has the ability of either promote or inhibit fuel oxidation, depending on the reaction conditions. In the gas-phase, the inhibition mechanism involves radical removal through:

$$K + OH + M \leftrightarrow KOH + M \quad (10)$$

$$KOH + H \leftrightarrow K + H_2O \quad (11)$$

However, reactions (10) and (11) can be reversed if the radical levels are low, resulting in a promotion of reaction by K [54]. Subsequently, after its release into the gas-phase, the K species can interact with other compounds through different reactions depending on the given reaction environment. These reactions will be responsible for the known ash-related issues of slagging, deposition and corrosion on the heating and cooling surfaces. The common reaction assumed to be responsible for the initial deposit formation is the KCl(g) condensation but, in absence of chlorine and sulfur, possible gas-phase reactions include the interaction of K(g) with water vapor to form KOH(g) and the subsequent carbonation of the hydroxide at temperatures below 1073 K [55]:

$$2\ KOH(g) + CO_2(g) \leftrightarrow K_2CO_3(g) + H_2O(g) \quad (12)$$

followed by the deposition of K_2CO_3(g) to K_2CO_3(s). The deposition of K_2CO_3 occurs generally on the cooling surfaces since K_2CO_3(s) is fully decomposed at 1123 K [56]. Other route for an initial deposit mechanism on cooling surfaces includes the directly condensation or deposition of KOH(g) to KOH(l,s) followed by:

$$2\ KOH(l,s) + CO_2(g) \leftrightarrow K_2CO_3(s) + H_2O(g) \quad (13)$$

Calcium can be found in biomass in three forms: organically bound, acid-soluble and acid-insoluble. Under combustion conditions, acid-insoluble Ca (e.g. Ca-silicates) is usually considered inert, whereas organically bound and acid-soluble Ca are readily converted into CaO [6]. As seen in the previous section, a large fraction of calcium is present in the biomass as CaC_2O_4, through which the thermal decomposition of its monohydrate form is described by the following reactions:

$$CaC_2O_4{\cdot}H_2O\ (s) \leftrightarrow CaC_2O_4\ (s) + H_2O\ (g) \quad (14)$$

$$CaC_2O_4\ (s) \leftrightarrow CaCO_3\ (s) + CO\ (g) \quad (15)$$

$$CaCO_3\ (s) \leftrightarrow CaO\ (s) + CO_2\ (g) \quad (16)$$

The temperature intervals at which each reaction occurs are 373-473 K, 673-803 K and 873-1083 K for reactions (14), (15) and (16), respectively [56,57]. Within the combustion chamber, CaO exists as refractory small micrometer-sized particles, and will stay as it is, provided it is not participating in further reactions [16].

1.3.3 IGNITION STUDIES

The study of ignition of pulverized solid fuels is an important subject due to flame stability, formation and emission of pollutants, and flame extinction matters that are fundamental for controlling the combustion process [58]. This area has recently started to see a great development with the advent of more advanced diagnostic techniques, which allow the study of isolated particles, in conditions close to those verified in pulverized combustion systems. Typically, the study of the ignition of biomass particles has been done using Drop Tube Furnace (DTF) reactors or Entrained Flow Reactors (EFR). The former allows a greater flexibility regarding the atmosphere composition where the particles are introduced, however the heating rates obtained with this equipment (10^4 K s^{-1}) [59] are lower than those typically found in pulverized industrial systems (10^5−10^6 K s^{-1}) [60]. The EFR allows obtaining conditions similar to those verified in industrial burners of pulverized fuels, regarding the heating rates and atmosphere composition. It also allows applying optical techniques to determine the combustion and ignition characteristics of pulverized fuels. In the majority of the works developed in the area of ignition of solid fuel particles, particle jets have been used. The study of single particle ignition only appeared more recently. There is currently a variety of equipment and techniques used to determine the ignition characteristics of a solid fuel, and due to this there is no method or universal definition of the ignition criteria. Thus, the results obtained are somewhat dependent on the technique and equipment used, and the comparison between the several studies should take these differences into account [61,62]. There have been a few attempts to study the ignition behaviour of single particle biomass fuels; however, they are still scarce when compared with studies done with coal, so in this section some studies regarding ignition of particles of coal will be addressed, namely regarding the development of the techniques to characterize the ignition behaviour (ignition delay and ignition mode).

Ignition criterion

Howard and Essenhigh [63,64], in the first works in this area in the 1960s, studied the ignition of bituminous coal particles in a vertical DTF. The authors collected solid samples along the vertical axis of the furnace using a suction probe, analyzing the loss of volatiles and ash and, consequently, the loss of fixed carbon. The ignition criterion was defined based on the loss of volatiles and fixed carbon in the initial moments of combustion. However, this study used intrusive techniques, and currently the optical techniques available, such as cinematography and pyrometry, allow characterizing the ignition process without disturbing the flow.

Still in the late 1980s and early 1990s, several authors began the study of ignition of solid fuels using optical diagnostic techniques like video cameras, photomultipliers and photodetectors and based

the ignition criterion on the luminous intensity captured during the early stages of the combustion. Wall et al. [61,65], in a DTF, took the light flash emitted from a continuous flow or pulse flow feeding of pulverized coal particles, observed with a video camera or a photomultiplier, respectively, as an indicator of the ignition event. Ruiz et al. [66], in a vertical laminar flow reactor, calculated the ignition delay time of a jet of coal particles based on the average jet velocity and the distance from the injector to the position where the ignition occurred. The distance was calculated by doing an average of three distinct methods: visual observation, video recording and temperature difference along the reactor with and without flame. For the two first methods, the ignition event was said to occur when the flame covered the cross section of the reactor, and for the third method when a 5 K increase in temperature was detected. Tomeczek and Wojcik [67] addressed the characterization of the ignition of a coal particle using a different installation and criteria. The authors used the gradient of luminous flux captured by a photodetector to determine the ignition event.

More recently, Shaddix and Molina [68], in a first work, addressed the topic of ignition of solid fuels, studying the ignition delay time of jets of bituminous coal particles in an EFR. The authors used a high-speed camera and a filter to capture a temporal mean of the CH* chemiluminescence emission of the coal particles, defining the ignition criterion as the beginning of CH* emission. The authors further attempted to capture the chemiluminescence of CH* for isolated particles but found it, however, very difficult to detect. In a second work [69], and using the same experimental setup, the authors applied a different ignition criterion, for isolated particles of bituminous coal. Three types of image (pre-ignition, devolatilization and char oxidation) were detected in which the fraction of each type of image varies with the residence time of the particle. The ignition criterion was defined based on these images in which the ignition delay time corresponded to the time between the injection of the particle in the reactor until the fraction of devolatilization images was equal to 50% of the total images. It was also defined that the devolatilization started when the emission intensity of the particle was greater than 60% of the maximum intensity in the image.

Levendis, Khatami, Riaza and co-workers [59,70–74] conducted several ignition studies in a DTF reactor with optical access. The optical access enabled the measurement of temperature-time-size histories of individual coal or biomass particles by three-color pyrometry and high-speed high-resolution cinematography. The authors defined the ignition criterion as the onset of the pyrometer signal or the first appearance of luminous combustion depending on technique used. The ignition temperature was defined as the first point where the maximum particle temperature gradient was recorded.

Yuan et al. [62], in an EFR setup, defined the ignition delay time as the time between the beginning of the injection of a jet of coal particles until the instant when 10% of the maximum luminous intensity was reached. Simões et al. [37] investigated the effect of temperature and oxygen concentration on the ignition of single particles of 5 biomass fuels in an EFR apparatus, namely a flat flame McKenna burner. In order to characterize the ignition, the authors determined the ignition delay time based on a criterion of 15% of the maximum luminosity intensity captured during the burning of a single particle. The ignition criterion was further refined in a following work [75] to 5% of the maximum luminosity intensity by applying a digital filter that could increase the signal-to-noise ratio and still maintain the most important characteristics of the combustion process.

Effect of gas temperature

The effect of gas temperature on the ignition behaviour of coal fuels has already been investigated in the literature [62,76]. Only recent works addressed this topic for biomass fuels. Magalhães [77], in a McKenna flat flame burner (EFR), studied the effect of gas temperature on the ignition delay time of single particles of pine bark, wheat straw and bituminous coal. It was concluded that by increasing the gas temperature, the ignition delay time of biomass particles decreases indicating that ignition occurs earlier, which is a result similar to those obtained for coal. Magalhães [77] also found that at high temperatures the biomass fuels present similar ignition delay times, which points toward a convergence of the ignition delay times at high heating rates revealing that the biomass composition and particle diameter become less important at high heating rates. This conclusion was later confirmed by Ferreira [75] that studied the ignition behaviour of single particles of other biomass and coal fuels, again using a McKenna flat flame burner, and compiling the data with the data obtained by Simões et al. [37]. These authors also verified that for wheat straw large particles the ignition mode changed from surface to gas-phase with increasing gas temperature conditions, which may be due to an increase in the devolatilization rate followed by an increase in the volatile flux that prevents the oxygen from reaching the surface of the particle, therefore, a volatile flame forms and lifts from the surface.

Effect of O_2 concentration

Again, the effect of O_2 concentration on the ignition behaviour has been widely studied for the case of coal particles, but little work has been done for biomass. Riaza et al. [59] studied the ignition behaviour of biomass particles, in a DTF, in air and oxy-fuel conditions (mole fractions of 21% O_2, 30% O_2, 35% O_2 and 50% O_2 in CO_2). The authors observed that the ignition delay time decreased with increasing O_2 concentration, the volatile flame decreased its brightness, whereas the char particle emitted stronger radiation and appeared brighter.

Simões et al. [37] also studied the effect of O_2 concentration on the ignition behaviour of 5 biomass fuels. The conditions used were obtained by changing the flow rates of air and methane supplied to the flat-flame McKenna burner to hold the same temperature and three different dry oxygen concentrations in the ignition zone (3.5, 5.1 and 6.5 vol.%). The results revealed that the ignition was predominantly occurring on the gas-phase mode, but for particles of wheat straw and vine branches there was a slight tendency to decrease the relative frequency of gas-phase ignition and increase the frequency of surface ignition with increasing O_2 concentration. It was also observed that the ignition delay time slightly decreased with increasing O_2 concentration for all biomass residues, which can be explained by an increase in the reactivity of the local fuel-oxidizer mixture. However, Ferreira [75] by studying the effect of O_2 concentration on the ignition delay time of almond shell, olive residue and two lignites, using three distinct operating conditions, obtained approximately uniform ignition delay times. Ferreira [75] also verified that the ignition occurs mostly on the gas-phase mode and no significant change was noticed with increasing O_2 concentration.

Effect of biomass type

There have been very few attempts to study the ignition behaviour of single particle biomass fuels and studies focusing on the effect of the biomass type on particle ignition are rather scarce [37,59,78]. Riaza et al. [59] investigated in a DTF the combustion behaviour of four pulverized biomass fuels (sugarcane bagasse, pine sawdust, torrefied pine sawdust and olive residue) in air and oxy-fuel atmospheres. The authors observed that sugarcane bagasse presented a longer devolatilization time and a shorter char burnout time compared with the other biomass fuels, being these results attributed to the higher volatile matter content and lower fixed carbon content in this biomass fuel, respectively. The authors also compared the combustion behaviour of biomass with the previously studied combustion behaviour of coal particles verifying that the combustion behaviour of biomass fuels did not change much with the different sources of biomass, unlike the combustion behaviour of coal that varies widely with rank, type and seam.

Mason et al. [78] studied the duration of the combustion stages of three biomass fuels (pine, eucalyptus and willow) on a Meker burner, observing a tendency for the ignition delay time to be higher for the solid fuels with higher moisture content. Simões et al. [37] studied the ignition behaviour of five biomass fuels (wheat straw, kiwi branches, vine branches, sycamore branches and pine bark) using an optical flat flame McKenna burner, and concluded that, for temperatures of 1500 and 1650 K, particle shape plays a more important role than the biomass composition on the ignition mode, and that the biomass composition has a higher impact on the ignition delay time for temperatures of 1500 and 1650 K than for temperatures of 1700 and 1800 K.

1.4. OBJECTIVES

The aim of this work is to investigate the impact of the presence and concentration of K and Ca on the devolatilization and char oxidation characteristics of biomass fuels, taking as reference point grape pomace biomass. The reference biomass was demineralized and subsequently doped with different concentrations of K and Ca, making a total of 12 different samples. This thesis is divided in two main parts, according with the type of experiments done, which in turn are closely related to the heating rates applied:

- In a first part, the impact of K and Ca on the pyrolysis and combustion behaviour of biomass at low heating rates using thermogravimetric analysis (TGA) is examined in order to understand the processes and reactions involved during devolatilization and char oxidation. The characteristic temperatures of the initial stage, of the peak rate, and of the final stage were compared for the different biomass samples.

- With the aim of extending the study to conditions closer to those of practical applications, raw, demineralized and impregnated biomass particles were fed, as single particles, to a confined

laminar flow of combustion products produced by a McKenna flat flame burner. This apparatus allows submitting the particles to high heating rates of around 10^5 K/s and provides optical access to study the early stages of combustion, namely ignition and volatiles combustion. First, the raw, demineralized and impregnated biomass particles were tested under two distinct temperature conditions to evaluate the effect of the presence of K and Ca on the ignition delay time. Subsequently, one of the conditions was chosen to evaluate the effects of the presence of those minerals on the volatiles combustion time. Finally, the ignition delay time variations were compared to the volatiles combustion time variations in order to evaluate the relative importance of the catalytic effects of the K and Ca in both phases.

1.5. THESIS OUTLINE

This thesis is divided in six chapters. In the present chapter, a general framework, a literature survey of previous studies and the main objectives of this study were established. The second chapter describes the experimental apparatus, methods, and associated uncertainties during measurements. In the third chapter, the results and respective discussion are presented. The chapters 4, 5 and 6 present the conclusions, future perspectives and references for this work, respectively.

2. MATERIALS AND METHODS

2.1. BIOMASS PREPARATION

In this study, grape pomace biomass has been selected as the reference biomass. Grape pomace is a residue generated during the wine production and it is mainly constituted by skins and seeds. The biomass was grinded using the laboratory-scale mill *Retsch SM 100* with a sieve of 1-mm-diameter and sieved with the aid of a *SS-15 Gilson Economy 203 mm Sieve Shaker* using sieves of 200 and 250 μm. Figure 2 shows the raw grape pomace sample after sieving. The particle size distribution, shown in Figure 3, was measured using the *Malvern 2600 Particle Size Analyzer*.

Figure 2. Grinded and sieved grape pomace sample in the size range 200-250 μm.

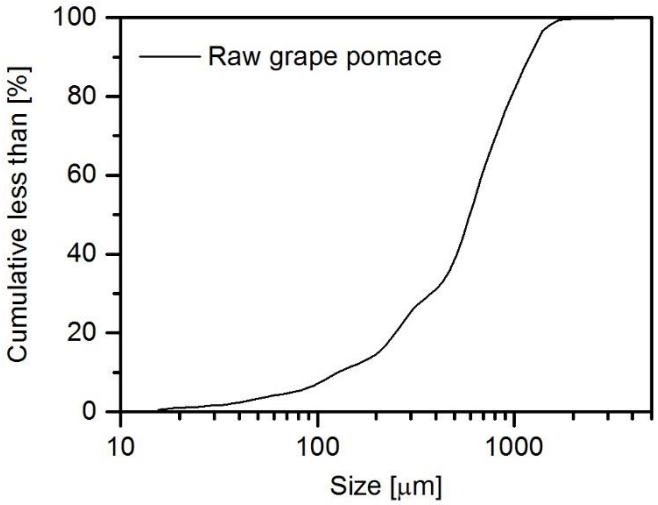

Figure 3. Grinded grape pomace particle size distribution.

The biomass was analyzed at the Centre for Wastes Valorization at the University of Minho, in accordance with the appropriate standards. The proximate analysis complied with the following standards: CEN/TS 15414:2006, CEN/TS 15402:2006, and CEN/TS 15403:2006. As far as the ultimate analysis was concerned, this was done according to CEN/TS 15104 and sulfur determined according to

CEN/TS 15408, the heating values were determined according to CEN/TS 14918:2015, and the chemical composition of ashes was determined by X-Ray fluorescence spectroscopy. Table 1 lists the main properties of the grape pomace biomass.

Table 1. Properties of the raw grape pomace biomass.

Parameter	Value
Proximate analysis (wt.%, as received)	
Volatiles	48.4
Fixed carbon	18.6
Moisture	30.2
Ash	2.8
Ultimate analysis (wt.%, dry ash free)	
Carbon	51.1
Hydrogen	6.7
Nitrogen	1.9
Sulphur	0.2
Oxygen	40.1
Heating value (MJ/kg)	
High	21.2
Low	19.8
Ash analysis (wt.%, dry basis)	
SiO_2	5.5
Al_2O_3	1.0
Fe_2O_3	1.2
CaO	37.8
SO_3	1.7
MgO	7.2
P_2O_5	19.7
K_2O	24.7
Na_2O	0.4
Cl	<0.01
Other Oxides	0.8

Comparing the proximate analysis of grape pomace with typical values of other biomass residues, it can be observed that grape pomace presents a higher moisture content (30.2 wt.% compared with a mean of 19.3 wt.% for wood and woody biomass residues and 12.0 wt.% for herbaceous and agricultural biomass residues as measured). It can also be observed that grape pomace has a slightly higher ash content than the average value for wood and woody biomass residues (mean 2.7 wt.% as measured) and lower than the average value for herbaceous and agricultural biomass

residues (mean of 5.1 wt.% as measured) [11]. It's important to note that biomass is characterized by having high heterogeneity, meaning that these average values may differ even for biomass of the same type.

By looking at the values obtained from the ash analysis, it is possible to observe that the concentrations of K and Ca in form of oxides are quite high in comparison with other elements, which is in agreement with the average values for wood and woody biomass residues and herbaceous and agricultural biomass residues, with exception of silica that is also in high concentrations in average for these biomass residues [11].

To prepare the different samples, the raw grape pomace was firstly demineralized by a nitric acid leaching procedure in order to remove the inorganic elements present [43]. This procedure consists mainly on 4 steps: sample and solution preparation, stirring, filtration and washing and, finally, drying. In particular, 30 g of raw biomass were placed in a flask with 500 ml of ion-exchanged water. The pH of the dissolution was adjusted to 2 using HNO_3 and stirred for 1 h at 60 °C. Subsequently, the biomass was filtered and washed thoroughly with 200 ml of ion-exchanged water. The filtering-washing procedure was repeated 4 times. Finally, the biomass was dried at 105 ºC. The complete procedure was repeated twice. A schematic to illustrate the process is represented in Figure 4.

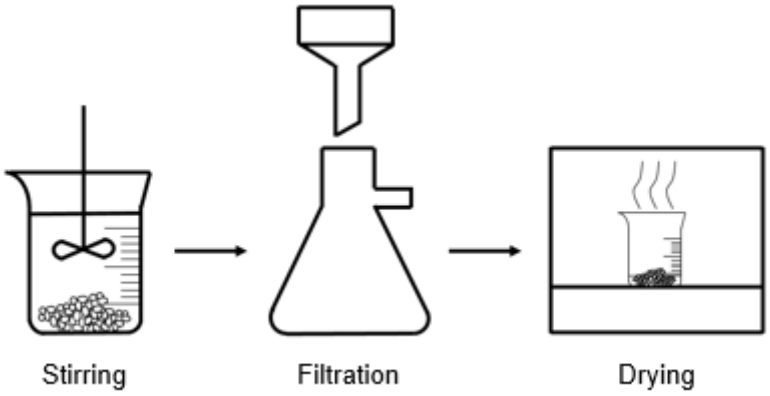

Figure 4. Demineralization process of biomass.

Afterwards, the demineralized biomass was impregnated with different concentrations of either K (using potassium oxalate monohydrate as reactant) or Ca (using calcium oxalate monohydrate as reactant). The wet impregnation procedure consists of adding different amounts of K or Ca reactant to 11 ml of ion-exchanged water and their subsequent mixture with 5 g of demineralized biomass. The resultant impregnated biomass samples were dried at 105 °C, and stored at ambient conditions.

The specific K and Ca reactant amounts were selected to cover a wide and realistic range of K and Ca concentration in different biomass residues [15]. Thus, a total of 12 different samples were obtained; specifically, raw grape pomace, demineralized grape pomace and impregnated grape pomace with 0.1, 0.5, 0.82 (equal to the K concentration in the raw biomass), 3 and 6 wt.% of K, and 0.1, 0.5, 1.08 (equal to the Ca concentration in the raw biomass), 3 and 6 wt.% of Ca.

Scanning electron microscope images were obtained from an *EDX Hitachi S-3400 N SEM microscope* with variable pressure up to 270 Pa and an *EDX Röntec XFlash analyzer of Si (Li)* analyzer.

Energy-dispersive X-ray spectroscopy (EDS) enabled to analyse the particle surfaces and to identify the elements present on a specified area with sufficient concentrations to be detected.

2.2. EXPERIMENTAL SETUP

2.2.1 THERMOGRAVIMETRIC ANALYZER

The evaluation of the combustion behaviour of biomass is based on the measurement of the mass change in a sample as a function of the temperature and time at a constant heating rate of 10 K/min from room temperature up to 1275 K in either nitrogen or air, using a *Netzsch STA F1 Jupiter* thermogravimetric analyzer (Figure 5).

Figure 5. *Netzsch STA F1 Jupiter* thermogravimetric analyzer.

The experiments were performed at atmospheric pressure using alumina crucibles and 5 mg of each biomass sample. The initial sample mass and heating rate used in these tests were chosen based on previous studies addressing the pyrolysis and combustion behaviour of different biomass residues in TGA experiments [79]. Prior to the experiments, for each experimental condition (i.e. air atmosphere or N_2 atmosphere), a calibration curve was made to avoid possible fluctuations caused by the apparatus that could influence the measurements.

The mass loss rate, dX/dt (min^{-1}) is defined as:

$$\frac{dX}{dt} = \frac{1}{m_0} \cdot \frac{dm}{dt} \tag{17}$$

where m_0 and m are the initial mass of biomass and the mass of biomass at time t in the TGA tests, respectively. Thus, the biomass conversion, X, is defined as:

$$X = \frac{m_0 - m}{m_0} \tag{18}$$

The experiments were repeated at least three times. In addition, to disregard the possible influence of the biomass size distribution on the TGA results, the samples were sieved into the 200-250 μm size interval and, subsequently, subjected to the pyrolysis and combustion tests. As an example of the data repeatability obtained, Figure 6 shows the conversion X and the rate of mass loss dX/dt for the pyrolysis of the demineralized biomass. The similitude of results is high, indicating a good repeatability of the procedure and a low effect of the biomass size distribution of the samples under the conditions of the present work.

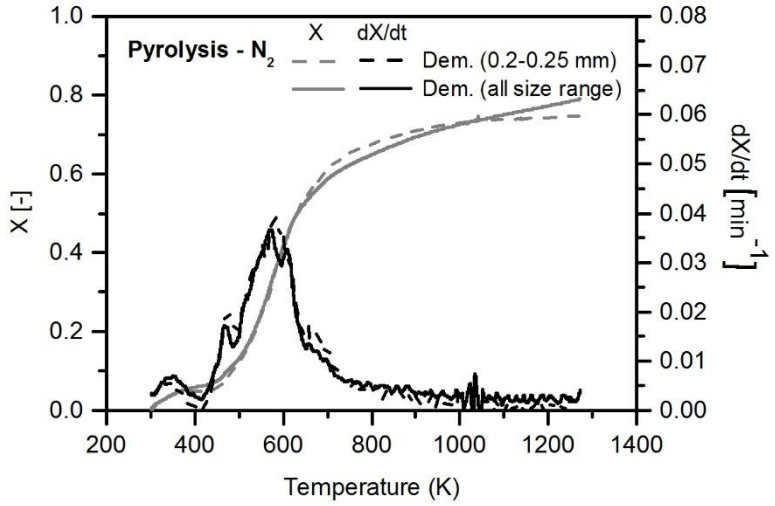

Figure 6. Typical pyrolysis profiles of the demineralized grape pomace.

2.2.2 IGNITION SETUP

Figure 7 shows the schematic of the ignition setup. It consists of McKenna flat flame burner, a biomass feeding unit, a gas feeding system, and an image acquisition system. The McKenna flat flame burner consists of a stainless-steel cylinder containing a water-cooled bronze porous sintered matrix of 60 mm diameter with a central hole of 1.55 mm internal diameter. Figure 8 shows the flat flame McKenna burner used in this work.

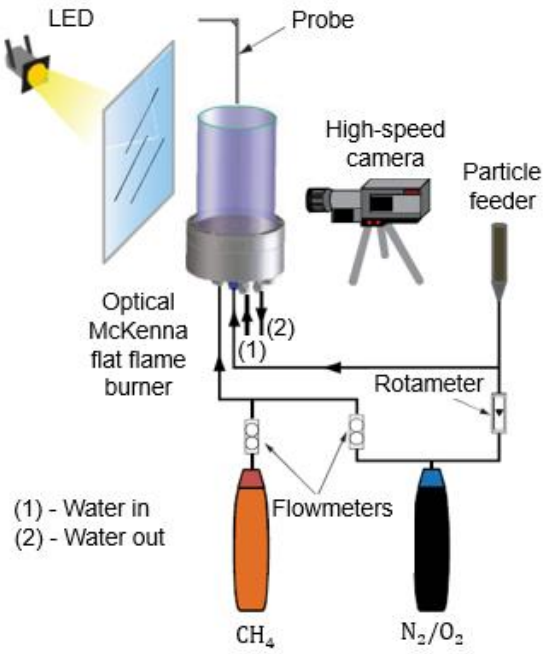

Figure 7. Schematic of the ignition setup.

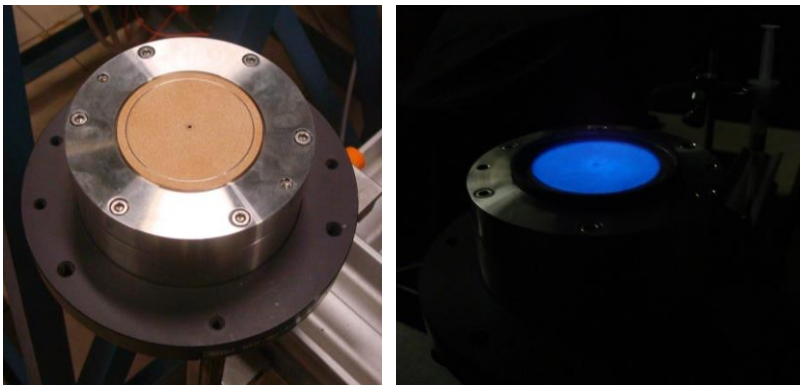

Figure 8. Flat-flame McKenna burner.

The flat flame is created above the sintered matrix by a premixed mixture of primary air flow and methane flow supplied to the burner by the gas feeding system. Two mass flowmeters are used to control the flow rates. Furthermore, to cool the sintered matrix, water is supplied through copper tubes. A high-grade fused quartz with an internal diameter of 70 mm, a height of 500 mm and a thickness of 2 mm, is used in order to confine the combustion products flow, and prevent the entrainment of ambient air while providing optical access. The biomass feeding unit, shown in Figure 9, includes a 10 ml syringe where the biomass particles are stored, a fine mesh, and a rotameter to regulate the transport air flow. The biomass particles are added to the transport air stream by gravitational force and injected upward

through the central hole of the burner. The fine mesh placed inside the syringe ensured a low feeding rate of particles allowing the recording of single particle videos.

Figure 9. Biomass feeding system.

The image acquisition system includes a CMOS high-speed camera Optronis CamRecord CR600x2, shown in Figure 10, equipped with a lens AF Micro-Nikkor 60 mm f/2.8D and a teleconverter Kenko TelePlus MC7 AF 2.0X DGX to increase the focal length of the lens used. Additionally, the image acquisition system includes a diffuse led backlight to enable the camera to record the shadow projection of the particles. In order to align the position of the camera, a target with millimeter marks was used for calibration before and after each experimental session. The axis of the camera was aligned perpendicularly with the axis of the burner so that the camera could record images of the particles since their injection. Table 2 lists the main camera settings used. A detailed description of the experimental setup used can be found elsewhere [37].

Figure 10. CMOS high-speed camera.

Table 2. Main camera settings.

Parameter	Setting
Aperture	2.8-5.6
Exposure time	1/8000
FPS	2300
Resolution [pix]	200×752

2.3. EXPERIMENTAL METHODS AND UNCERTAINTIES

The equipment used to supply air and methane to the McKenna burner was an *Atlas Copco GX7ff* compressor with a capacity of 10 bar and an industrial cylinder of 200 bar, respectively. Two controllers were used to control the gas flow rates (Figure 11). For the primary airflow, an *Aalborg* mass flow meter with an operating range of 0-50 dm^3/min, at 25 °C and 1 atm, was used, and for the methane a *Tylan General* controller with an operating range of 0-50 dm^3/min, at 25 °C and 1 atm. In order to control the transport air flow rate, a flowmeter with an operating range of 0-0.34 dm^3/min, at 25 °C and 1 atm, was used, which makes possible to measure very low flow rates with good precision. The flow rates were unaffected by temperature and pressure variations within the operating conditions of the equipment (0-50 °C 1-70 bar). The associated uncertainty of these equipments is +/- 2%.

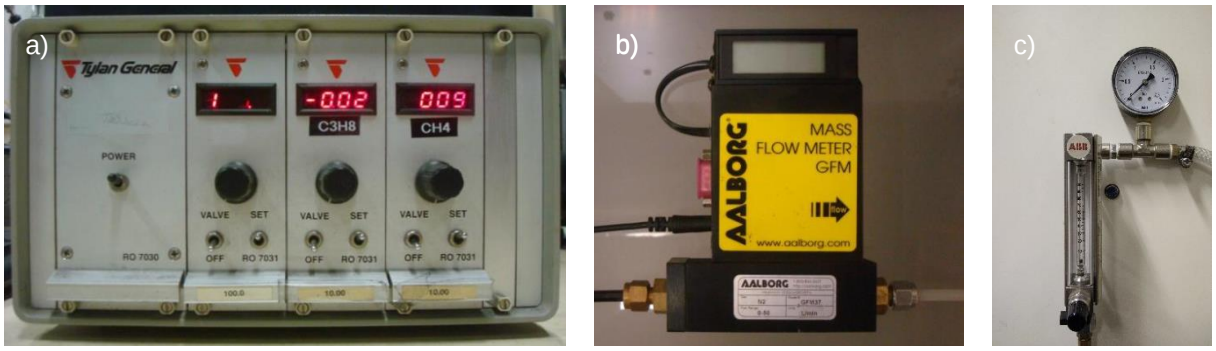

Figure 11. a) Methane controller, b) Primary air mass flow meter c) air transport rotameter.

The primary air controller was calibrated for N_2, so it was necessary to calibrate it for air. The methane flow rate was also verified. This calibration was done using the soap bubble technique, which consists in measuring the time that a gas flow takes to move a soap bubble through a chosen volume. The equipment used to perform this technique was a soap bubble flow meter. The calibration curves for the primary air and methane flow rates are shown in Figure 12. The equation of the trend line is given in the figures together with the squared correlation coefficient (R^2). Each point of the plot was obtained by measuring the time that the primary air or methane flow takes to move a soap bubble through the volume defined in the flowmeter. Ten measured times were taken and an average was made for each

measured point. The trend line was obtained by linear regression and the actual values of the gas flow rates used were extrapolated from that. These values were then verified by measuring the values of oxygen with the aid of probe at the exit.

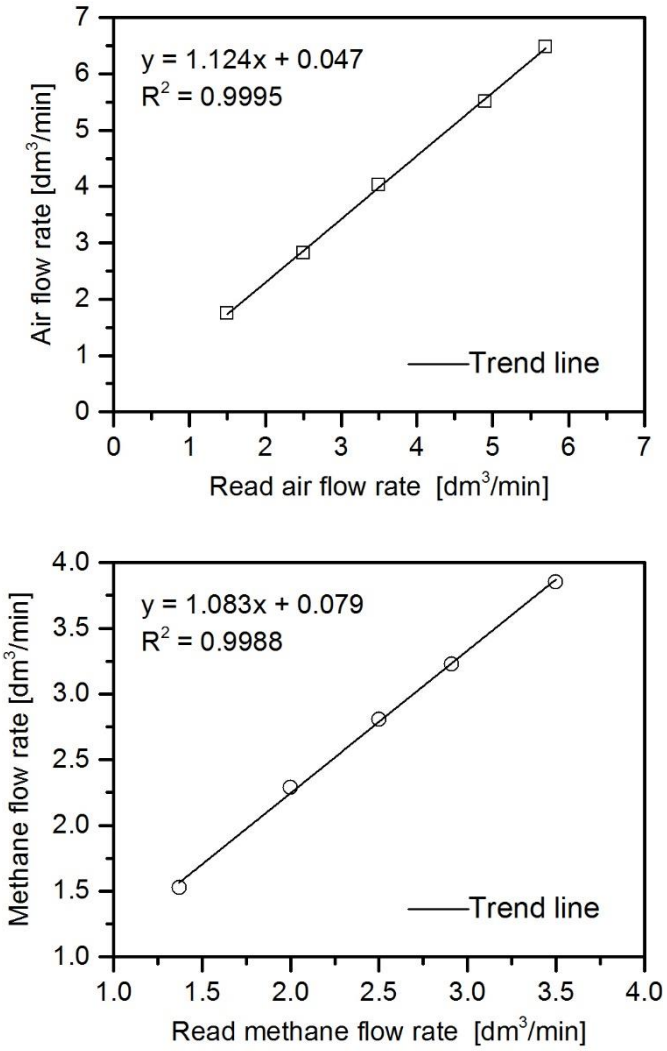

Figure 12. Calibration curves for a) primary air mass flow meter and b) methane controller, at 25 °C and 1 atm.

Temperature measurement

The gas temperature measurement profiles along the axis of the burner were measured using a probe with a 76 µm R-type thermocouple. Figure 13 shows a schematic of the probe. This thermocouple consists of 13% rhodium platinum/platinum uncoated wires that were welded using resistance electric welding. The welded wire was then wrapped around two other wires of the same material having a diameter of 350 µm leaving the welded joint stretched and centered relative to the two wires. These two wires were enclosed in a double-hole ceramic structure to be protected. The thermocouple used operates within the temperature range of 223 and 2041 K. To carry out the

temperature measurements, the probe is positioned on a mechanical arm that allows movement in three directions, allowing the positioning of the thermocouple in the desired position with an accuracy of ±1 mm. Temperatures at each position were read for 30 seconds from a computer where a data acquisition board is attached, which receives the potential difference created by an electromotive force generated by the temperature difference between the thermocouple ends. Each temperature profile was repeated three times in order to obtain error bars.

There are some particularities related to temperature measurement through thermocouples that have to be taken into account and that may affect the accuracy of the measurements obtained. According to [80] these sources of error are of aerodynamic, thermal or chemical nature. They are associated with induced perturbations in the flow by the probe, contamination of thermocouple wires that can induce chemical reactions on its surface, catalytic effects and conduction and radiation heat transfer errors. Due to the laminar nature of the combustion products flow in the McKenna burner, the disturbances induced by the probe in the flow are neglected.

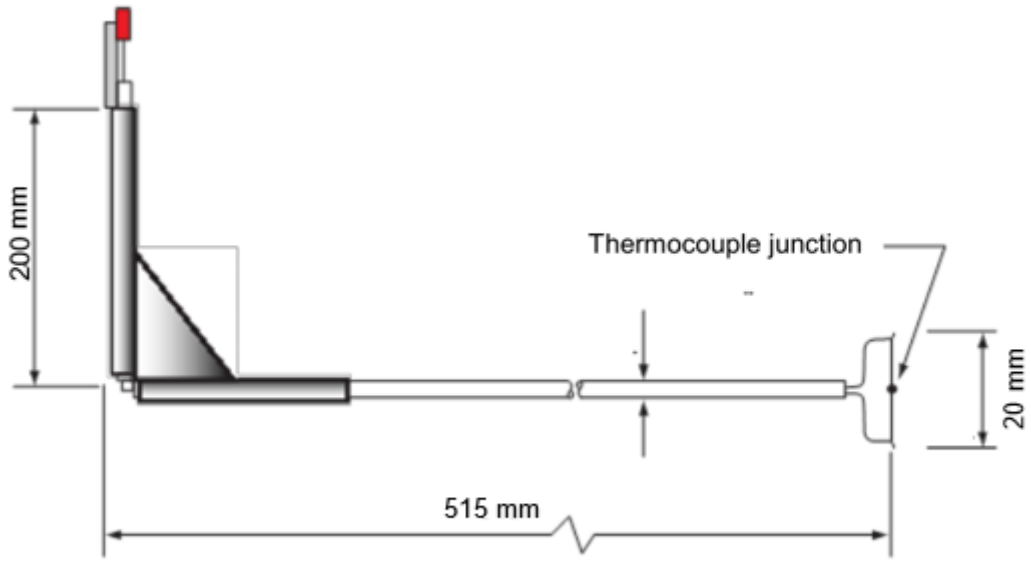

Figure 13. Thermocouple probe used.

The values of the temperature measured represent the temperature of the thermocouple bead and not the gas temperature. The gas temperature can be estimated by doing an energy balance on the thermocouple bead. In steady-state conditions the energy balance is given by:

$$\dot{Q}_{cond} + \dot{Q}_{conv} + \dot{Q}_{rad} + \dot{Q}_{cat} = 0 \tag{19}$$

where $\dot{Q}_{cond}$, $\dot{Q}_{conv}$ and $\dot{Q}_{rad}$ are the terms of heat transfer by conduction, convection and radiation respectively. The term $\dot{Q}_{cat}$ corresponds to the heat transfer associated with the induced catalytic reactions. The terms $\dot{Q}_{cat}$ and $\dot{Q}_{cond}$ are very difficult to quantify and estimate and are significantly smaller than the terms $\dot{Q}_{conv}$ and $\dot{Q}_{rad}$, so they were not considered in the analysis. To determine $\dot{Q}_{conv}$

a Nusselt number correlation to determine the convection coefficient was used, as recommended by Shaddix [81]. To estimate $\dot{Q}_{rad}$ some assumptions were done: the gas atmosphere was considered transparent and the thermocouple was assumed to have a gray, diffuse surface. The bead was split into two surfaces in which the upper surface emits radiation to a distant large black surface at ambient temperature and the bottom surface absorbs radiation emitted by a hot circular black surface (hot flame). A detailed description of the energy balance and the assumptions made can be found in [32].

Measurement of species concentration

To characterize the flow of combustion products of air and methane in the flat flame burner a water-cooled stainless steel probe mounted on a mechanical arm was used to collect samples of the major chemical species, namely, O_2, CO_2, CO, NO_x and HC. Figure 14 shows the probe used. The probe collects the gas sample continuously with the help of a diaphragm pump and a rotameter that controls the suction flow rate. Then the sample passes through a condenser where the moisture and particles that may be in the sample are removed, thereby promoting the constant supply of clean and dry gas sample to the analyzers. The sample also passes through a dryer and a filter that complement the function of the condenser. After drying, the sample reaches the analyzers, which measure the concentration of the gas species in volumetric percentage on a dry basis. The analog signals obtained from the analyzers are subsequently converted into digital through analog-to-digital converters and shown in a computer. The values are measured during 30 seconds and the mean value calculated. The connection between the probe and the analyzers and all connections of the remaining components are done through a chemically inert material (PTFE) in order to avoid the contamination of the gas sample. The analyzers are calibrated before and after each run with standard mixtures. Each sampling test was repeated three times.

The uncertainties associated with the measurements are attributed to the insufficient quenching of the chemical reactions, the disturbance of the flow through due to the presence of the probe, which may lead to non-isokinetic suction and catalytic effects on the probe surface. In order to prevent the condensed water on the surface of the probe from falling into the burner by gravity, the suction must be increased, which, on one hand, may increase the cooling, helping quenching the reactions, but, on the other hand, the suction ceases to be isokinetic, which may represent a high uncertainty in the measurements taken. However, the flow of combustion products is laminar with a constant radial profile, so these uncertainties can be neglected for the measurement of the concentration of the gas species.

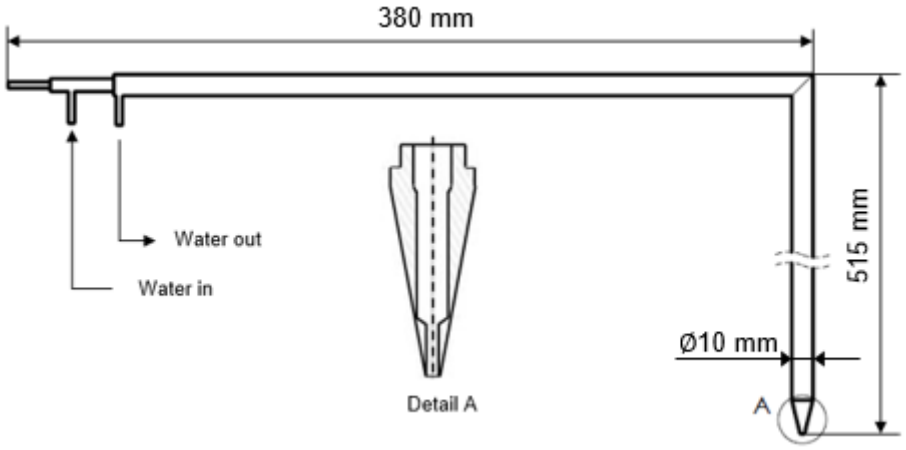

Figure 14. Gas species sampling probe used.

Table 3. List of analyzers.

Species	Analyzer	Scale	Analysis method	Standard mixture
O_2	Horiba, Model CMA-331 A	0-25%	Paramagnetism	20.9%
CO_2	Horiba, Model CMA-331 A	0-50%	Non-dispersive infrared sensors	12.3%
CO	Horiba, Model CMA-331 A	0-50/5000 ppm	Non-dispersive infrared sensors	100 ppm
NO_x	Amluk, Model FID E 2020	0-1000 ppm	Chemiluminescence	92 ppm

2.4. POST PROCESSING OF DATA

The images collected with the high-speed camera were examined in order to calculate the ignition delay time and the volatiles combustion time, using a method previously developed by Simões et al. [37]. Capturing the visible light from the particles has been proved to be a good indicator of ignition despite soot and char emissions being included in the visible light captured [62,69]. Figure 15 shows a typical original and filtered (post-processed) normalized signal. Single particles burned almost exclusively in sequential form (97% of the samples), i.e., volatiles combustion followed by char combustion as shown in the figure, which allowed measuring the duration of the volatiles combustion. The post-processing of the normalized signal consists in a filtering process that removes noise by smoothing the curve. Subsequently, an ignition criterion is used to find the frame in which the maximum pixel intensity is closest to the intensity defined by the ignition criterion. Volatiles combustion starts at the ignition point and ends at the local minimum as shown in Figure 15.

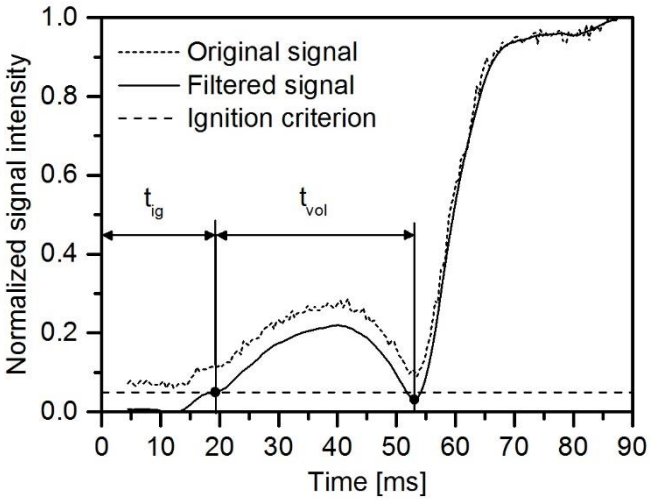

Figure 15. Original and filtered normalized signal.

In this work, the filtering process was improved to allow for a better signal-to-noise ratio and a reduction of the ignition criterion from 15% to 5% of the maximum luminosity intensity. The filtering process consists mainly on three steps: a noise attenuation step, a translation step, and a normalization step. In the noise attenuation step, a robust local regression was applied to the light signal using weighted linear least squares and a second order polynomial regression. This method was chosen due to its simplicity and flexibility. A detailed description of the smoothing procedure can be found elsewhere [82]. The translation step consisted on the removal of the background noise from the original signal, by subtracting the minimum signal value to the original signal, and the normalization step normalized the scale of the signal to the maximum pixel intensity found in each recorded set of frames for a single particle. The post processing steps are illustrated in Figure 16.

Figure 17 shows a typical example of the statistical convergence of the ignition delay time and volatiles combustion time for one biomass sample. In the case of the ignition delay time, a minimum of 50 single particle ignition events for each biomass sample were analysed in order to identify the number of ignition events necessary to have statistical convergence. In the case of the volatiles combustion time, a minimum of 30 single particle events were analyzed for each biomass sample.

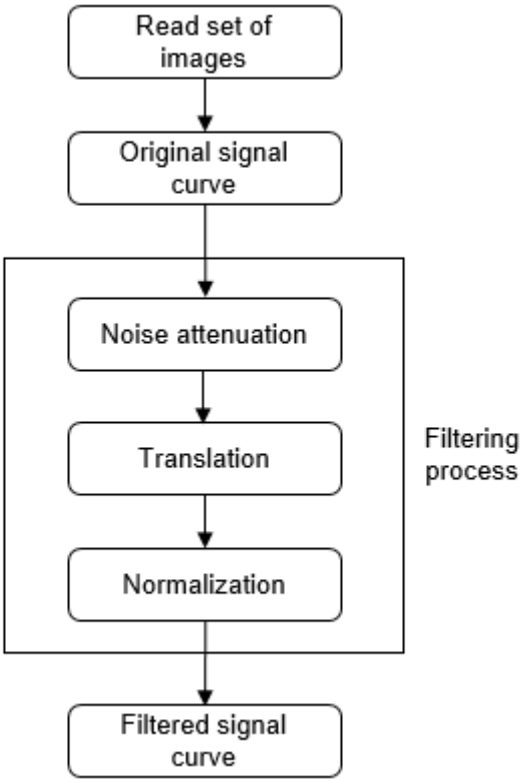

Figure 16. Post processing processes to obtain the filtered signal curves.

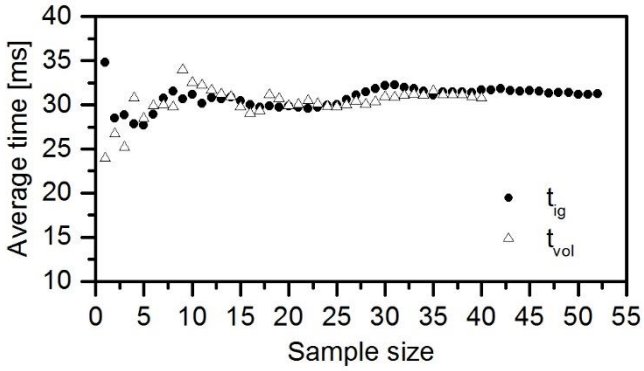

Figure 17. Example of the statistical convergence of the ignition delay time and volatiles combustion time.

3. RESULTS AND DISCUSSION

3.1. BIOMASS CHARACTERIZATION

The process of demineralization using acidic solutions is known to introduce alterations in the morphological structure of biomass. The acquisition of images from a scanning electron microscope (SEM) allows seeing these changes. Figure 18 shows the SEM images for the raw, demineralized and impregnated grape pomace samples.

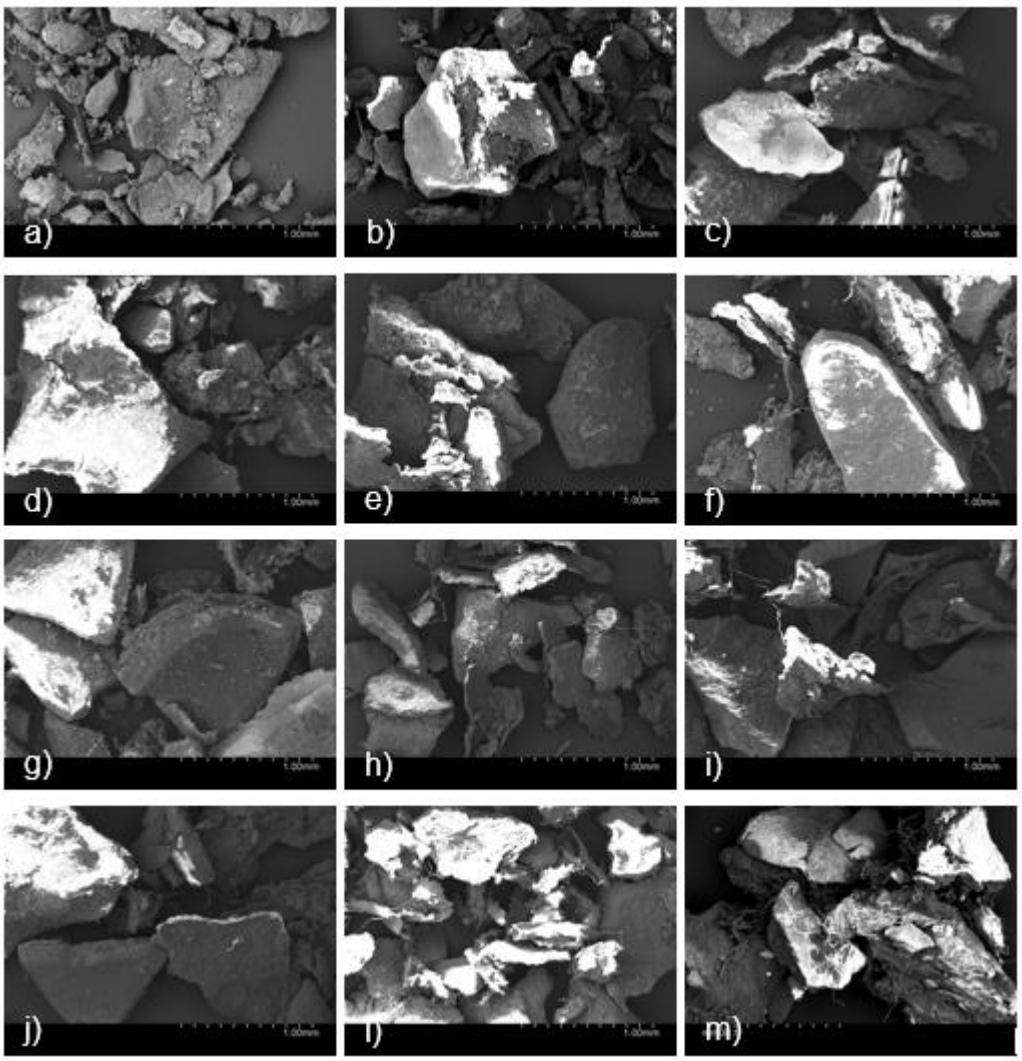

Figure 18. SEM images: a) raw grape pomace sample; b) demineralized grape pomace; sample impregnated with c) 0.1 wt.% Ca; d) 0.5 wt.% Ca; e) 1.08 wt.% Ca; f) 3 wt.% Ca; g) 6 wt.% Ca; h) 0.1 wt.% K; i) 0.5 wt.% K; j) 0.82 wt.% K; l) 3 wt.% K and m) 6 wt.% K.

Through these SEM images, it is possible to observe that the pre-treatments of demineralization and impregnation with the elements K and Ca did not introduce significant differences in the morphological characteristics at the surface of the biomass .

Energy-dispersive X-ray spectroscopy (EDS) analysis allowed to identify the elements present on the surface of the several samples, and it was verified that in the demineralized sample no AAEM species were found and that the concentration of the elements K and Ca in the biomass increased with increasing concentrations of these elements during impregnation. It is important to note that this is only a qualitative analysis, since elements with low atomic number, such as hydrogen, are not detected by this method.

3.2. THERMOGRAVIMETRY RESULTS

Figure 19 shows the conversion, X, and the conversion rate, dX/dt, *versus* temperature of the raw grape pomace and the demineralized grape pomace during the pyrolysis and combustion processes.

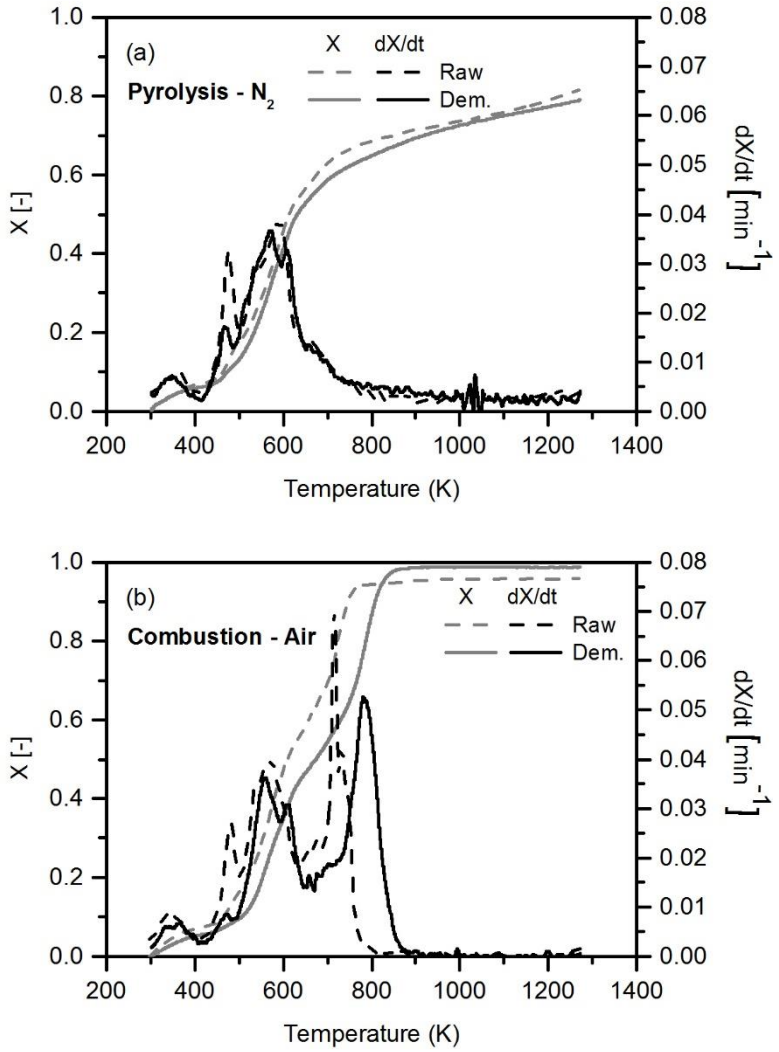

Figure 19. a) Pyrolysis in N_2 and b) combustion in air of raw and demineralized grape pomace up to 1275 K at 10 K/min in TGA.

The pyrolysis conversion profile of both biomass samples (Figure 19a) is characterized by an initial rapid decomposition, in the 425-650 K temperature interval, followed by a slower process up to a biomass conversion of about 0.8 at 1275 K. Despite the initial rapid decomposition being associated with an intense volatile matter release, the volatile matter release occurs during the whole process, even in a later stage where it becomes residual being this stage attributed to a slow decomposition of the char in biomass.

The combustion conversion profile (Figure 19b) shows two rapid conversion stages separated by a gradual transition stage. For both the raw and demineralized grape pomace, the volatile matter release stage is finished at around 675 K. However, the char conversion stage is finished at 800 K for the raw biomass and at 875 K for the demineralized biomass, pointing to a catalytic effect of metals during the char oxidation process. The demineralized biomass was fully consumed during its interaction with air (0.99 conversion), whereas the maximum conversion for the raw biomass is 0.96. This difference is attributed to the ash content of the raw grape pomace (cf. Table 1), and supports the effectiveness of the demineralization process.

Figure 19 also shows the pyrolysis and combustion rates. After the first peak at 350 K that corresponds to the water release, for both the pyrolysis and combustion processes, the raw grape pomace devolatilization shows three distinct peaks for the pyrolysis process (Figure 19a). These peaks are generally associated with the release of the three main biomass components: hemicellulose (at 498-598 K), cellulose (at 598-648 K) and lignin (at 523-773 K) [14]. In Figure 19b, for the combustion rate curve of raw grape pomace, the first two peaks occur at similar temperatures as the peaks of the raw grape pomace pyrolysis rate curve. However, this curve exhibits a third peak, which is very intense and stronger than the other peaks, associated with the char oxidation.

The pyrolysis rate curve corresponding to the demineralized biomass shows the three peaks at the same temperature as in the case of the raw biomass, pointing to a marginal effect of the ash constituents of grape pomace on the characteristic temperatures of the volatile matter release. However, the magnitude of the peaks is slightly affected by the biomass demineralization treatment. The magnitude of the first peak, associated with hemicellulose, is the most affected. It substantially decreases when the biomass is demineralized. Previous studies [39,83] indicate that the demineralization processes, such as water or mild acid washing can separate and sharp the peaks of the rate curves. In the present work, the hemicellulose peak from the demineralized biomass is significantly decreased, up to almost disappear, presumably due to its chemical degradation during the acid demineralization [48].

In the combustion rate curve of the demineralized sample, the hemicellulose peak also decreased when compared with the raw sample, showing the same behaviour observed in the pyrolysis rate curves. The char oxidation peak decreased its intensity and was shifted to higher temperatures when the biomass was demineralized, reinforcing the catalytic effect of metals on char combustion.

To establish how the reactivity of the biomass is affected by the presence and concentration of K and Ca, the pyrolysis and combustion rates from the demineralized biomass are taken as reference. Figures 20 and 21 show the rate of mass loss for the demineralized grape pomace and all the K and Ca doped biomass samples considered in this work during their pyrolysis and combustion, respectively.

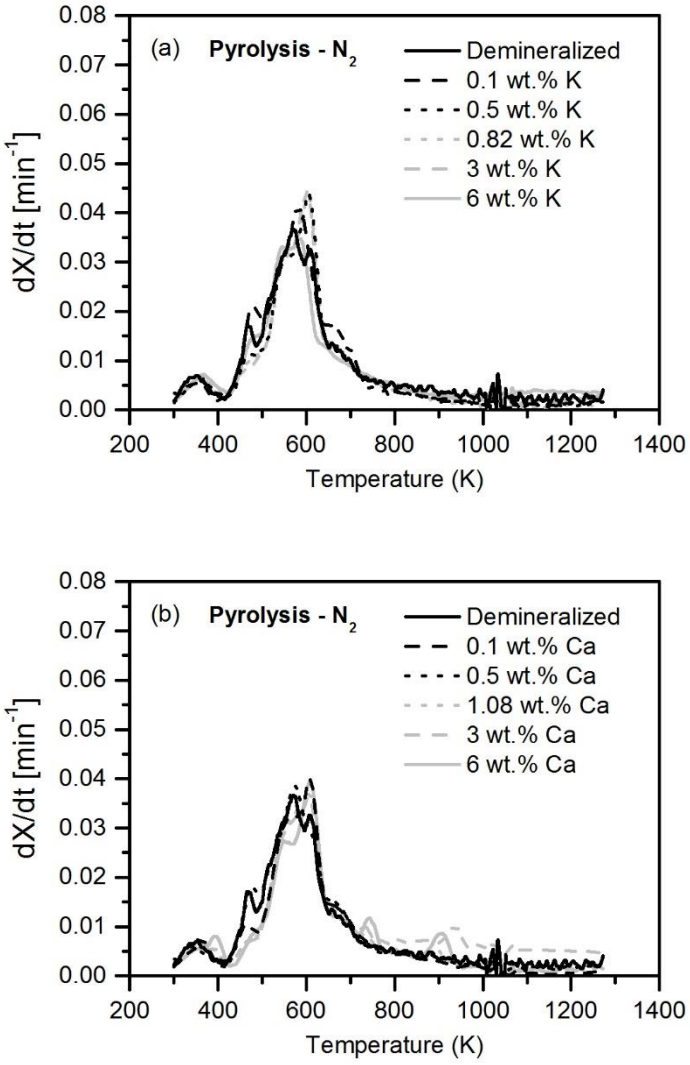

Figure 20. Pyrolysis profiles of demineralized grape pomace and grape pomace doped with the different concentrations of K (a) and Ca (b).

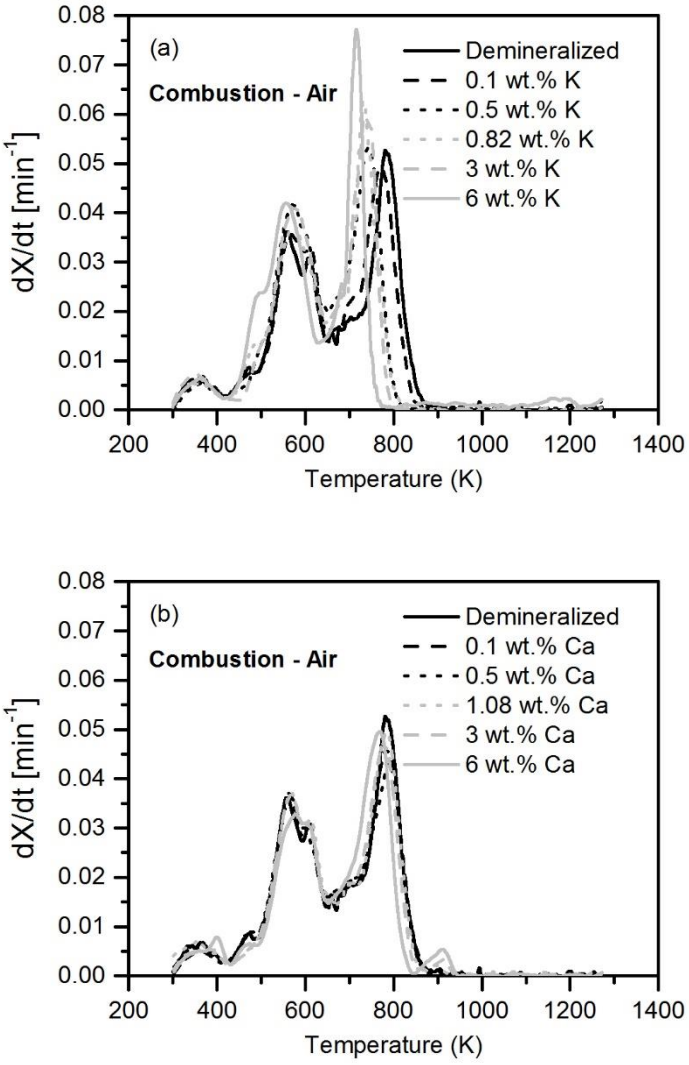

Figure 21. Combustion profiles of demineralized grape pomace and grape pomace doped with different concentrations of K (a) and Ca (b).

The general biomass pyrolysis profile (Figure 20) is neither influenced by the K nor by the Ca content. Independently of the K and Ca contents, the volatile matter release stage takes place in the 425-650 K temperature interval, with the main devolatilization peak within this range. In the case of the Ca doped biomass samples, especially for the samples with 3 and 6 wt.% of Ca, the dX/dt profile shows two distinct peaks, at ~750 and ~925 K, respectively, that can be associated with the Ca transformations at high temperature. The reactant used in the present work to dope the demineralized biomass with Ca is calcium oxalate monohydrate ($CaC_2O_4 \cdot H_2O$). Its thermal decomposition involves dehydration, decomposition of calcium oxalate to calcium carbonate ($CaCO_3$) and the further decomposition of the calcium carbonate to calcium oxide (CaO) [56,57]. Therefore, the characteristic peaks obtained would correspond to the decomposition of CaC_2O_4 to $CaCO_3$ and the subsequent formation of CaO. It is also interesting to note that the magnitude of the CaC_2O_4 and $CaCO_3$ decomposition peaks decreases as the amount of Ca used during the impregnation of the biomass decreases. For the K doped biomass

samples, the pyrolysis dX/dt profile does not show any additional peak associated with the presence of K or its concentration. As indicated in the introduction section, during a thermochemical process potassium is released to the gas-phase as K (g), while calcium is released as small micrometer-sized CaO particles, which would support the different observations above mentioned.

In the case of biomass combustion (Figure 21), the main devolatilization peak is affected by the K content, even though at a smaller extent, and it isn't significantly affected by the Ca content of the biomass. However, K and Ca play a different role on the char oxidation process. In general, the K content of biomass influences the char oxidation process by changing the temperature of its occurrence as well as its mass loss rate, whereas Ca does not significantly influence this process. The char oxidation peak temperature is progressively shifted to lower temperatures and its intensity increased as the K content of biomass is increased. For example, the peak temperature is shifted from 786 to 714 K with increasing the K content from demineralized biomass to 6 wt.% of K. It is important to note that it is not only the char oxidation peak that is shifted to lower temperatures as the K content increases. The initial and final temperatures of this stage also decrease, meaning that the whole char oxidation process is occurring at lower temperatures, as the K content in biomass increases. Table 4 summarizes the characteristic temperatures of the volatile matter release and char oxidation regions.

Table 4. Characteristic temperatures (K) of the devolatilization region of pyrolysis and the volatile matter release and char oxidation regions of combustion of the raw and demineralized grape pomace and doped with the different concentrations of K and Ca.

Biomass sample	Pyrolysis			Combustion					
				Devolatilization			Char oxidation		
	T_i	PT_{dev}	T_f	T_i	PT_{vol}	T_f	T_i	PT_{char}	T_f
Raw biomass	412	586	626	420	569	633	634	722	775
Dem. Biomass	420	576	646	418	565	656	657	786	875
0.1 wt.% K	400	583	637	420	572	652	653	772	853
0.5 wt.% K	420	607	640	418	572	647	648	743	821
0.82 wt.% K	420	607	637	420	572	641	642	736	825
3 wt.% K	422	600	635	432	575	647	648	736	800
6 wt.% K	420	586	626	418	558	631	632	714	775
0.1 wt.% Ca	420	607	643	430	565	645	646	786	878
0.5 wt.% Ca	415	572	641	424	569	652	653	793	878
1.08 wt.% Ca	420	604	644	424	568	670	671	786	868
3 wt.% Ca	424	607	640	428	569	649	650	779	860
6 wt.% Ca	426	608	646	430	579	654	655	768	843

T_i: initial temperature of the stage; PT: peak temperature; T_f: final temperature of the stage

3.3. EARLY STAGE COMBUSTION OF SINGLE PARTICLES

3.3.1 EXPERIMENTAL CONDITIONS

Two different operating conditions were used in this work, named here conditions T1 and T2. These conditions were established by varying the thermal input while maintaining constant the excess air coefficient, which made possible to obtain a mean temperature difference of approximately 200 K along the working zone. Also, during the experiments, the transport air flow rate was maintained very low (0.11 dm^3/min at 25 °C and 1 atm), which was the lowest flow rate tested that guaranteed single particle feeding. Table 5 lists the burner operating conditions used in this work.

Table 5. Burner operating conditions.

Parameter	**T1**	**T2**
Thermal input [kW]	0.9	1.8
Methane flow [dm^3/min] at 25 °C and 1 atm	1.5	3.2
Primary air flow [dm^3/min] at 25 °C and 1 atm	19.2	40.5
Transport air flow [dm^3/min] at 25 °C and 1 atm	0.11	
Excess air coefficient λ	1.3	
Mean gas temperature [K]	1575	1775
Mean O_2 concentration [dry vol.%]	5.4	5.2

Figure 22 shows the mean gas temperature and the mean O_2 concentration profiles for the test conditions used. This figure also includes the gas temperature profiles corrected for radiation losses using the method described in Simões et al. [37]. The temperature along the axis near the burner at 5 mm is lower due to the transport air flow, at ambient temperature, that goes in through the injection hole in the center of the burner. Then, this temperature increases as the height above the burner increases due to the mixture of the flows of transport air and combustion products, reaching its stabilization at a height of interest. Far away from the burner, the temperature starts to decrease due to heat losses. As the thermocouple moves away from the flame, the heat loss by radiation to the environment increases, and due to this, the estimated temperature becomes higher than the measured temperature.

In the case of the mean O_2 concentration profiles, these started at higher O_2 concentrations near the burner, due to the transport air flow that goes in through the injection hole, stabilizing when this flow mixes with the combustion products flow.

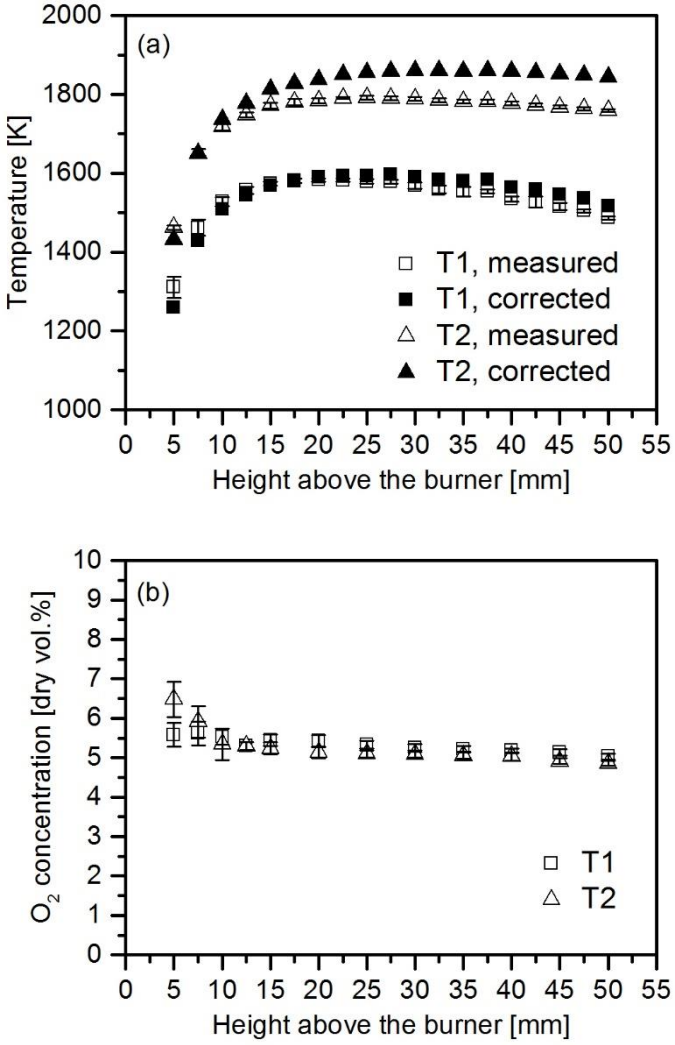

Figure 22. Mean gas temperature and mean O_2 concentration profiles for the operating conditions used.

3.3.2 EARLY STAGE COMBUSTION PROCESS

Figure 23 shows typical signal intensity curves of the combustion process of single particles as a function of time, and Figure 24 shows images of selected events marked in Figure 23. In Figure 23a) the original and filtered signal intensity curves are shown for a single particle of samples with 0.1 and 6 wt.% of K impregnated, whilst Figure 23b) shows the same curves but for samples with 0.1 and 6 wt.% of Ca impregnated.

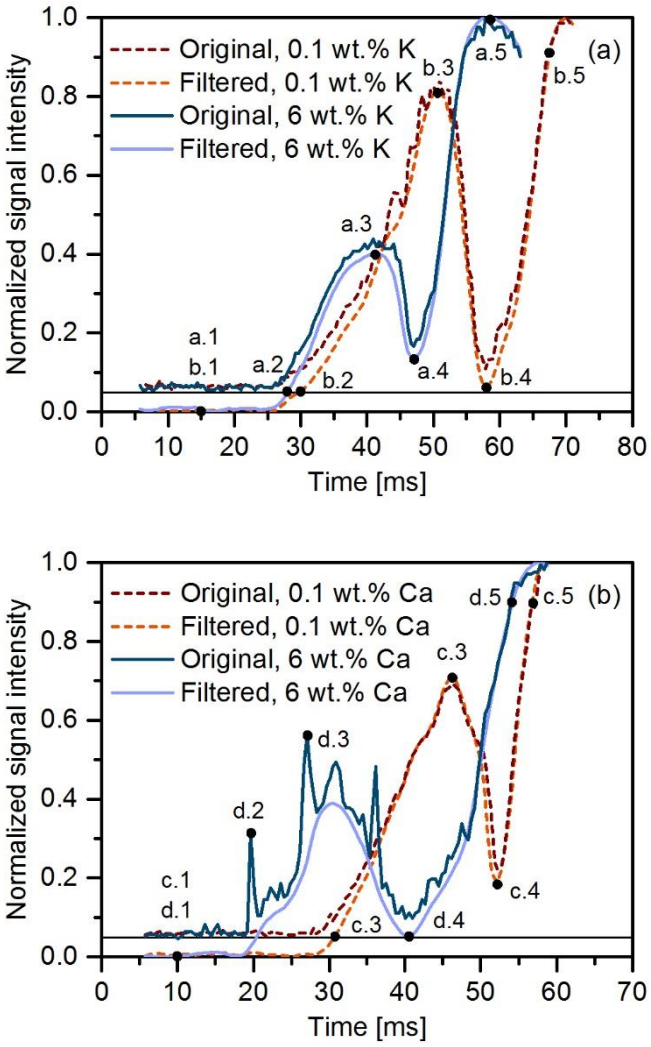

Figure 23. Signal intensity curves of (a) K impregnated samples; and (b) Ca impregnated samples.

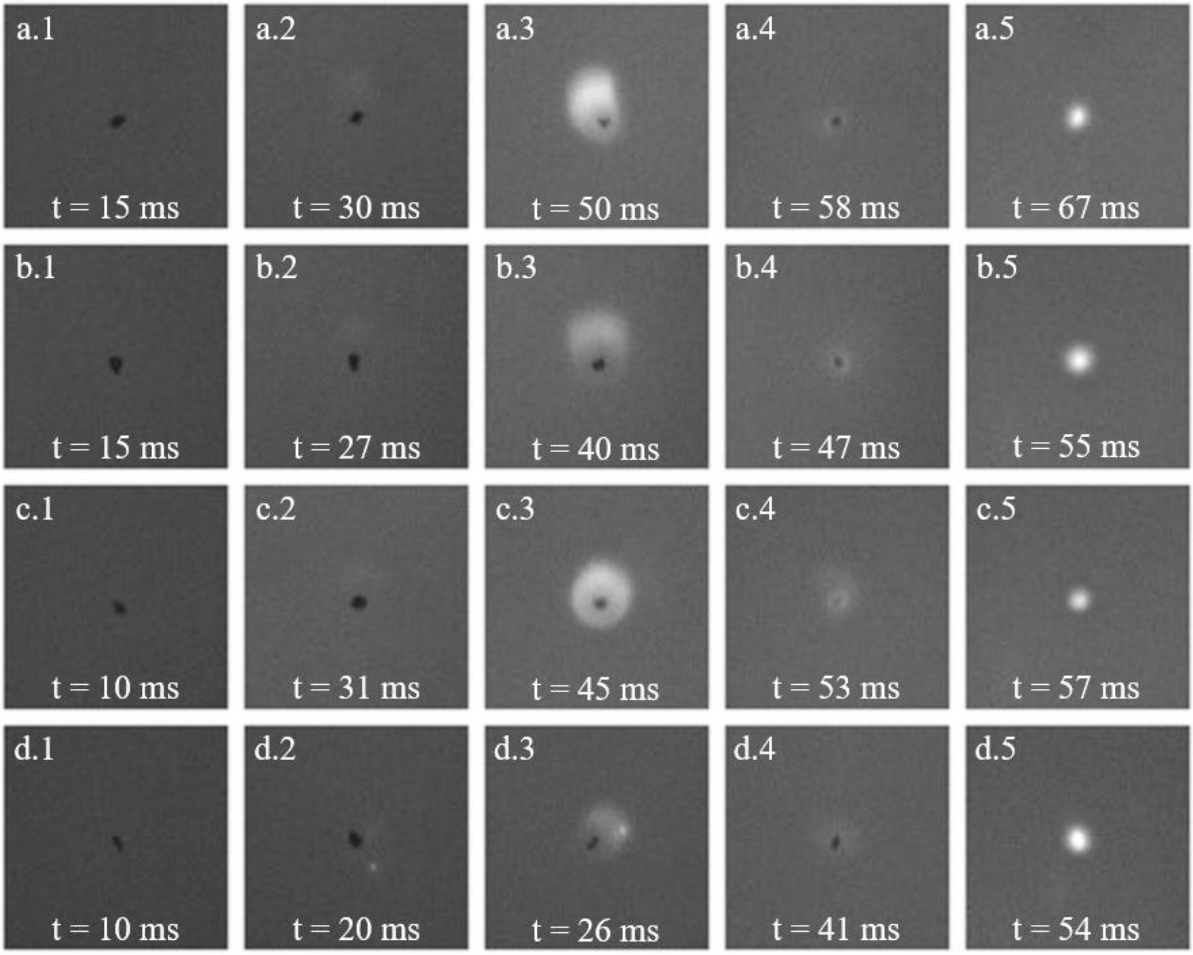

Figure 24. Images of selected events marked in Figure 23.

Each curve in Figure 23 presents similar characteristics for each phase of the combustion process varying only on the signal intensity and time values of each event. Taking the signal curves (original and filtered) of 0.1 wt.% K as an example, the signal intensity increases when ignition occurs (a.2). Subsequently, the signal intensity continues to increase due to the light captured from the volatiles flame around the particle until a local maximum is reached (a.3). Then, the signal intensity decreases until a local minimum is reached corresponding to a transition from the volatiles combustion to the char oxidation phase (a.4). In the char oxidation phase the particle surface glows brightly with a rapid increasing of the signal intensity (a.5). In some cases, the char oxidation may overlap the final stages of the volatiles combustion (c.4). In the case of the samples with 6 wt.% of Ca, very small glowing particles were ejected from the surface during the volatiles combustion (d.2 and d.3). As discussed in section 1.3.2 the calcium oxalate monohydrate forms CaO(s) through the following reaction sequence:

$$CaC_2O_4 \cdot H_2O\ (s) \leftrightarrow CaC_2O_4\ (s) + H_2O\ (g) \quad (14)$$

$$CaC_2O_4\ (s) \leftrightarrow CaCO_3\ (s) + CO\ (g) \quad (15)$$

$$CaCO_3\ (s) \leftrightarrow CaO\ (s) + CO_2\ (g) \quad (16)$$

CaO(s) is a refractory material that will be emitted as micrometer-sized particles provided it does not participate in further reactions [29]. As seen in Figure 22b), the filtering process was able to smooth the intensity peaks caused by the CaO(s) without compromising the shape of the signal curve.

The biomass particles size range considered is very small, thus it can be assumed that there are no internal temperature gradients (Bi << 1) and it has been reported in the literature that biomass particle temperatures during char oxidation phase in air combustion in a DTF may be 200-400 K higher than the atmosphere temperature of around 1400 K [59]. Even though the flame temperature during the volatile combustion phase was not measured, it has been reported temperatures of around 600 K above the atmosphere temperature in the case of coals [74]. Considering the flat flame McKenna burner, the particles enter in a hot flue gases environment of H_2O, CO and CO_2 compounds, at very high temperatures (mean gas temperature of 1575 K and 1775 K), meaning that the particle will be submitted to very high heating rates that may encourage the K and Ca mechanisms, presented in section (1.3.2), to occur during the volatile combustion phase or even before the onset of ignition. This explains why it was observed the release of CaO(s) micro-sized particles during and before the volatile combustion stage, through the thermal decomposition of $CaCO_3$ (16) at temperature range of 873 – 1083 K [56].

3.3.3 IGNITION DELAY TIME

Figure 25 shows the ignition delay time as a function of the K and Ca concentrations for both operating conditions T1 and T2. It is important to refer that the data points corresponding to zero concentration represent the demineralized biomass samples, and the hollow symbols represent the raw biomass samples. It is observed that the removal of the inorganic elements from the raw biomass causes an increase of the ignition delay time. Figure 25a) shows that the impact of the K on the ignition delay time. Two distinct regions can be observed: region I and II. In region I the ignition delay time decreases with the increase of the K concentration and an asymptote is reached around 1 wt.% of K, regardless of the operating condition. This asymptote remains until 3 wt.% of K, beyond which the ignition delay time decreases again (region II) for both operating conditions. Finally, the ignition delay time for the biomass sample with 0.82 wt.% (same K concentration as the raw sample) is very close to the ignition delay time of the raw sample of grape pomace for operating conditions T1 and T2.

Figure 25b) shows that the effect of the Ca on the ignition delay time differs from the effect of the K, although two regions can also be observed. In region I there is an increase of the ignition delay time from the sample with zero concentration of Ca until the sample with a Ca concentration similar to that in the raw biomass (1.08 wt.% in this case), regardless of the operating condition. The subsequent data points (3 and 6 wt.%) registered a decrease in the ignition delay time from the previous ones (region II) for operating conditions T1 and T2. Finally, the biomass sample with the same Ca concentration as the raw sample presents differences of 15% and 27% on the ignition delay times when compared with

the raw grape pomace sample, for the operating conditions T1 and T2, respectively. This result may indicate that the Ca present in the grape pomace biomass isn't responsible for decreasing the ignition delay time.

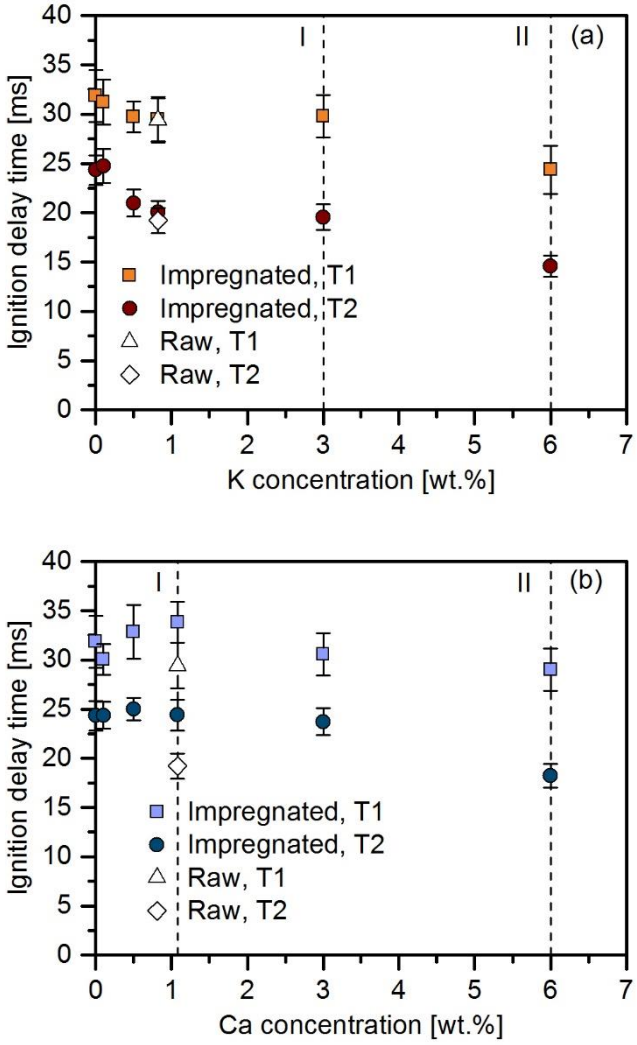

Figure 25. Ignition delay time as a function of the (a) K and (b) Ca concentration.

As for the effect of the temperature, it is observed that the ignition delay time of all samples decreases following a translation along the vertical axis, with no particular change in the gradients between the measured points. For this reason, only one operating condition was chosen for the evaluation of the volatiles combustion time.

3.3.4 VOLATILE COMBUSTION TIME

Figure 26 shows the volatiles combustion times as a function of the K and Ca concentrations for the operating condition T1. The figure reveals that the volatiles combustion time is much higher for the demineralized grape pomace sample than for the raw sample, with a difference of 24%, which means that the volatiles combustion time is strongly affected by the demineralization process.

Figure 26a) shows that the volatiles combustion time rapidly decreases as the concentration of impregnated K in the biomass samples increases up to a K concentration of 0.82 wt.%, beyond which it remains constant up to 6 wt.% of K. Nonetheless, it is important to note that the volatiles combustion time for the raw sample is lower than that observed for all samples with K impregnated which indicates that there are other variables that can influence the volatiles combustion of biomass and are not present in the pretreated samples. Figure 26b) shows that the evolution of the volatiles combustion time with the concentration of Ca impregnated in the biomass samples is similar to that of Figure 26a). As the impregnated Ca concentration increases the volatiles combustion time rapidly decreases until 1.08%, but in this case the asymptote is not reached up to a concentration of Ca of 6 wt.%.

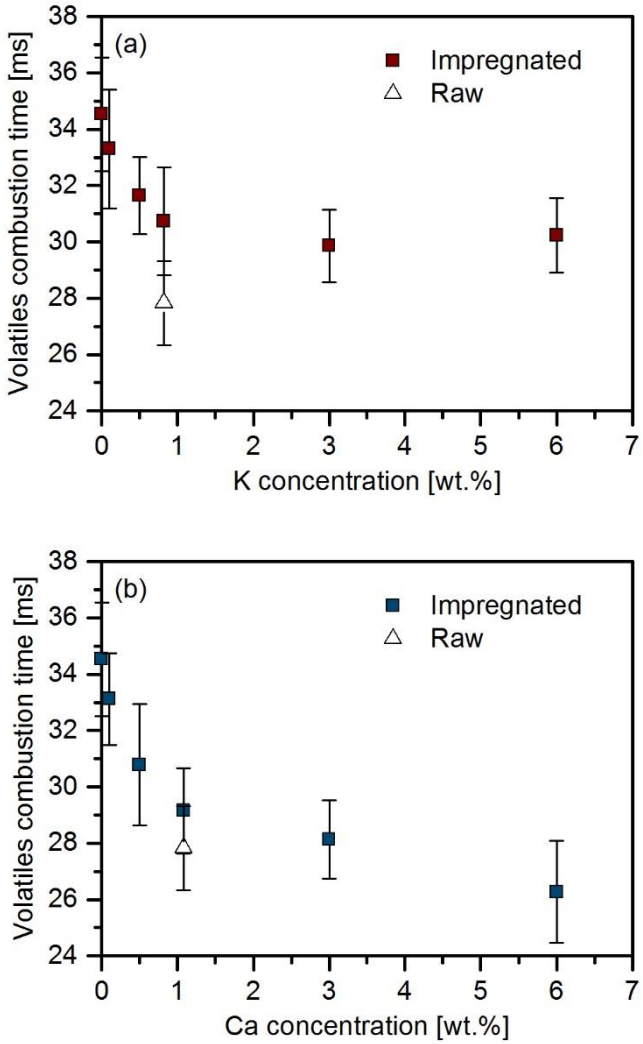

Figure 26. Volatiles combustion times as a function of the (a) K and (b) Ca concentration for the operating condition T1.

3.3.5 COMPARISON BETWEEN THE IMPACT OF K AND CA ON IGNITION DELAY TIME AND VOLATILE COMBUSTION TIME

Figure 27 shows the ignition delay time and volatiles combustion time differences between the demineralized and impregnated biomass samples with the same K and Ca concentrations as the raw biomass sample, and the raw biomass sample for the operating condition T1. It is seen that the demineralization has a negative impact on both the ignition delay time and the volatiles combustion time, with the strongest impact on the latter. Adding K to the demineralized sample reduced the ignition delay time to that observed for the raw sample. This action also reduced the volatiles combustion time, but to a smaller extent as compared with the raw sample. Adding Ca to the demineralized sample increased the ignition delay time, but reduced significantly the volatiles combustion time to a value close to that of the raw sample. In addition to Ca and K, the raw biomass contains other metals (cf. Table 1). These results suggest that neither K nor Ca are the sole responsible of the reduction in the volatiles combustion time observed for the raw biomass, at least not individually. However, K seems to be the main responsible for the lower ignition delay time of raw biomass, provided that synergy effects among ash constituents of raw biomass are negligible.

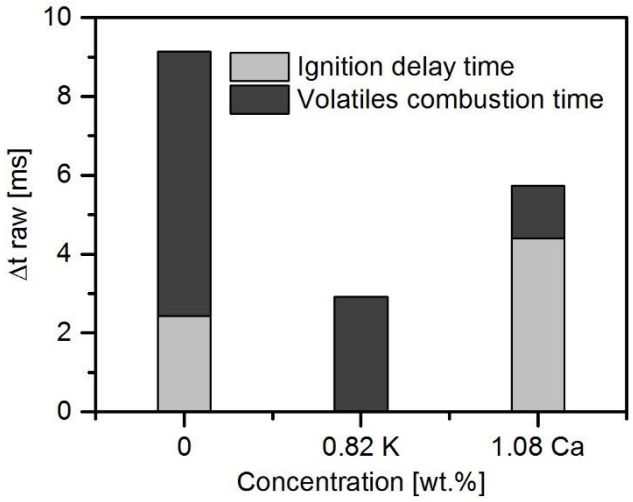

Figure 27. Ignition delay time and volatiles combustion time differences between the demineralized and impregnated biomass samples with the same K and Ca concentrations as the raw biomass sample, and the raw biomass sample for the operating condition 1.

Figure 28 shows the ignition delay time and volatiles combustion time differences between the impregnated biomass samples, with K and Ca, and the raw biomass sample for the operating condition T1. Generally, the effect of the K and Ca concentration is more significant on the volatiles combustion time than on the ignition delay time, especially in the case of the impregnation of Ca, being the only exception the sample with a concentration of 6 wt.% of K.

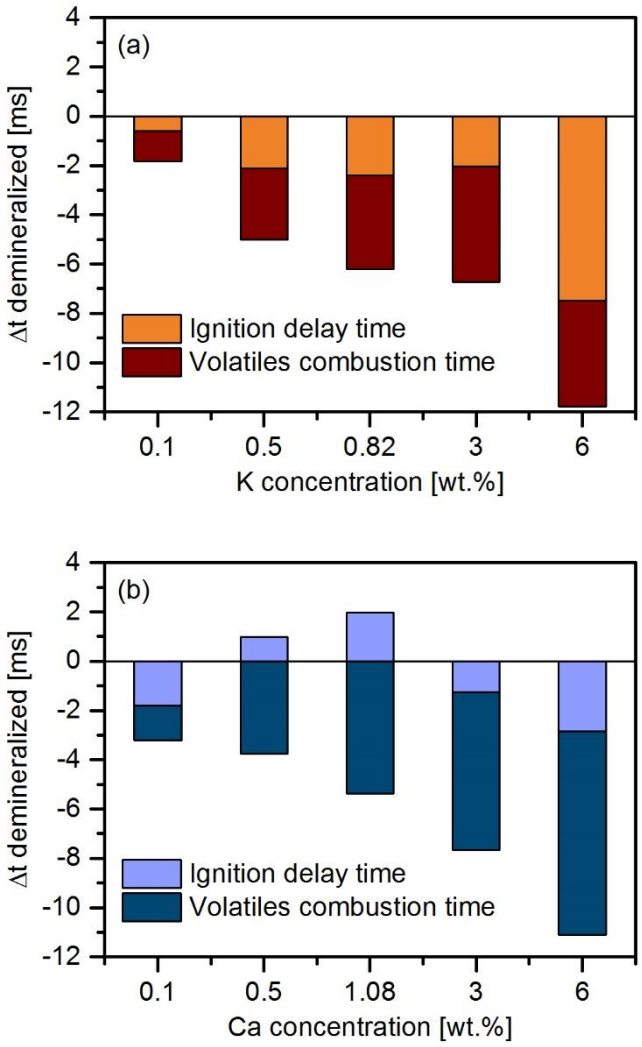

Figure 28. Ignition delay time and volatiles combustion time differences between the impregnated biomass samples and the raw biomass sample for the operating condition 1. (a) K and (b) Ca.

4. CONCLUSIONS

In this work, the effects of K and Ca on the pyrolysis and combustion behaviour of biomass were firstly examined, at low heating rates, using TGA, in order to understand the processes and reactions involved during devolatilization and char oxidation and which of these stages is more affected by the presence of K or Ca, by analyzing the mass loss and mass loss rate curves of each sample. Afterwards, a flat flame McKenna burner was used to determine the effect of K and Ca on the ignition delay time and volatiles combustion time of single particles of pre-treated biomass samples, at high heating rates. In order to carry these studies, regarding the influence of K and Ca on the combustion behaviour of biomass, the biomass used (grape pomace) was subjected to different pre-treatments. The first pre-treatment was the demineralization, which removed the inorganic present in the raw grape pomace allowing comparing and studying the influence of the inorganic matter present in the biomass. Through following pre-treatments of impregnation of an element of interest (K or Ca) with increasing concentrations, it was possible to study the effect of the particular element in the combustion behaviour of biomass. A total of 12 different samples were obtained, specifically, raw grape pomace, demineralized grape pomace and impregnated grape pomace with 0.1, 0.5, 0.82 (equal to the K concentration in the raw biomass), 3 and 6 wt.% of K, and 0.1, 0.5, 1.08 (equal to the Ca concentration in the raw biomass), 3 and 6 wt.% of Ca. The main conclusions of this work can be summarized as follows:

- In the TGA results, the demineralization process applied to the biomass decreased the hemicellulose peak during pyrolysis and shifted the DTG combustion profile to higher temperatures revealing that the mineral matter affects the combustion process of biomass. In the flat flame McKenna burner results, both the ignition delay time and the volatiles combustion time of single particles increased with the demineralization process, revealing a catalytic effect of the presence of the minerals on the early stages of the combustion process of the biomass particles.

- For the case of the element K, during combustion in TGA, by increasing the K concentration in the biomass, the devolatilization peak slightly increased whereas the char oxidation peak clearly increased. Additionally, the DTG profile was shifted to lower temperatures. In the flat flame McKenna burner experiments, both the ignition delay time and the volatiles combustion time of single particles decreased as the K concentration of the biomass sample increased. However, this decrease was more significant on the volatiles combustion time than on the ignition delay time, showing that K has a more pronounced impact on the volatiles combustion stage.

- For the case of the element Ca, during pyrolysis in TGA, in the curve associated with the impregnation of Ca, the peaks related to the thermal decomposition of $CaC_2O_4 \cdot H_2O$ increased with increasing Ca concentration in biomass. Also in TGA, increasing Ca concentration in the biomass had no significant influence on the DTG combustion profile. In the flat flame

McKenna burner results, the ignition delay time first increased and then decreased as the Ca concentration increased. Impregnated Ca, also had an impact on the volatiles combustion by decreasing its duration as the concentrations of impregnated Ca increased. Again, as in the case of K impregnation, the impact of Ca impregnation was more prominent in the volatile combustion time than on the ignition delay time.

To conclude, from the point of view of the ignition delay time and volatiles combustion time with the perspective of reaching flame stability, impregnation with low concentrations of K (up to 0.82 wt.%) would be viable. However, other relevant issues would arise and which were not discussed in detail, in this work, such as the ash-related issues. There must be an understanding and compromise between the improvement in the subject of flame stability and the ash-related problems introduced in the furnaces before applying the pre-treatment of impregnation.

5. FUTURE PERSPECTIVES

Ash release chemistry and formation is a complex subject and most of the studies focusing on the catalytic effect of AAEM during combustion have been done using TGA at low heating rates by measuring the mass loss and the mass loss rate of a given pre-treated sample. However, the study of these effects on single particle combustion behaviour at high heating rates is even more complicated. This work is a first attempt of studying this subject at high heating rates using a flat-flame McKenna burner based on the observations of the ignition delay time and volatile combustion time. A next step would be to study with more detail and try to understand the physical and chemical processes behind the catalytic effect of the AAEM on the combustion behaviour of single biomass particles, particularly the effect of potassium. To do so, more advanced optical equipment should be used, for instance pyrometry, spectrometry and cinematography, in order to understand the physical and chemical mechanisms involved during the initial stages of the combustion process and at what temperature they occur, in conditions similar to those verified in pulverized combustion systems. Based on a cooperation established with the Combustion Physics Division in Lund University, a follow up study was already initiated where advanced optical techniques are being used (see Figure 29).

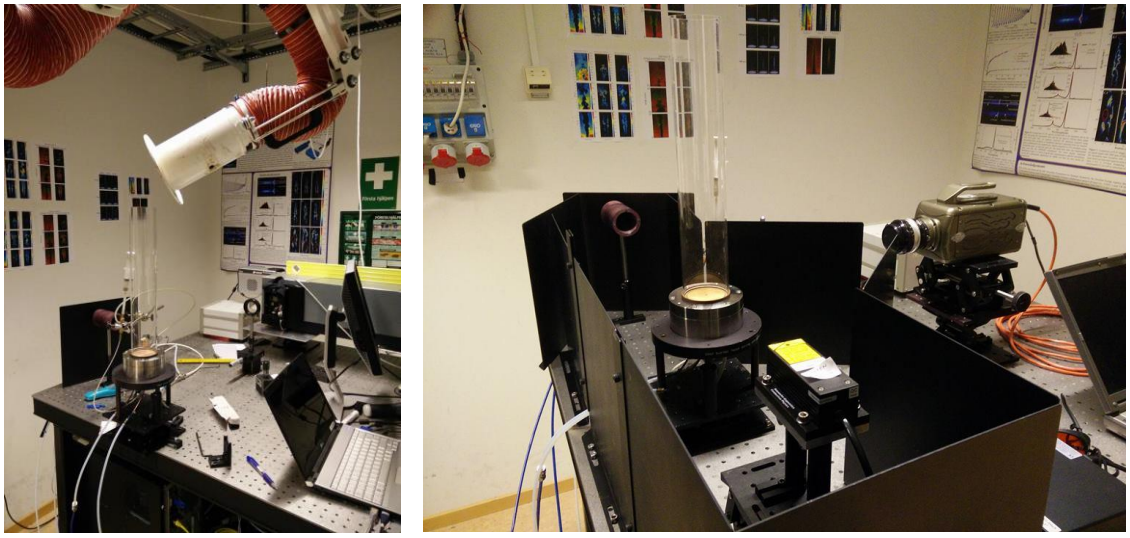

Figure 29. a) Spectrometry measurements of combustion of single biomass particles; b) ICCD measurements using filters to capture CH*, OH*, potassium and sodium emissions.

6. REFERENCES

[1] BP. BP Energy Outlook 2017 edition 2017.

[2] BP. BP Statistical Review of World Energy - Full report 2016:1–48.

[3] Mckendry P. Energy production from biomass (part 1): overview of biomass. Bioresour Technol 2002;83:37–46.

[4] Saidur R, Abdelaziz EA, Demirbas A, Hossain MS, Mekhilef S. A review on biomass as a fuel for boilers. Renew Sustain Energy Rev 2011;15:2262–2289.

[5] Al-Mansour F, Zuwala J. An evaluation of biomass co-firing in Europe. Biomass and Bioenergy 2010;34:620–629.

[6] Niu Y, Tan H, Hui S. Ash-related issues during biomass combustion: Alkali-induced slagging, silicate melt-induced slagging (ash fusion), agglomeration, corrosion, ash utilization, and related countermeasures. Prog Energy Combust Sci 2016;52:1–61.

[7] Demirbas A. Potential applications of renewable energy sources, biomass combustion problems in boiler power systems and combustion related environmental issues. Prog Energy Combust Sci 2005;31:171–192.

[8] Biagini E, Barontini F, Tognotti L. Devolatilization of biomass fuels and biomass components studied by TG/FTIR technique. Ind Eng Chem Res 2006;45:4486–4493.

[9] Olanders B, Steenari BM. Characterization of ashes from wood and straw. Biomass and Bioenergy 1995;8:105–115.

[10] Obernberger I. Ash related problems in biomass combustion plants. Inaug Lect 2005.

[11] Vassilev S V., Baxter D, Andersen LK, Vassileva CG. An overview of the chemical composition of biomass. Fuel 2010;89:913–933.

[12] Niu Y, Zhu Y, Tan H, Wang X, Hui S, Du W. Experimental study on the coexistent dual slagging in biomass-fired furnaces: Alkali- and silicate melt-induced slagging. Proc Combust Inst 2015;35:2405–2413.

[13] van Lith SC, Alonso-Ramírez V, Jensen PA, Frandsen FJ, Glarborg P. Release to the gas phase of inorganic elements during wood combustion. Part 1: Development and evaluation of quantification methods. Energy and Fuels 2006;20:964–978.

[14] Nunes LJR, Matias JCO, Catalão JPS. Biomass combustion systems: A review on the physical and chemical properties of the ashes. Renew Sustain Energy Rev 2016;53:235–242.

[15] Tortosa Masiá AA, Buhre BJP, Gupta RP, Wall TF. Characterising ash of biomass and waste. Fuel Process Technol 2007;88:1071–1081.

[16] Zolin A, Jensen A, Jensen PA, Frandsen F, Dam-Johansen K. The influence of inorganic materials on the thermal deactivation of fuel chars. Energy and Fuels 2001;15:1110–1122.

[17] Jiang L, Hu S, Sun L shi, Su S, Xu K, He L mo, Xiang J. Influence of different demineralization treatments on physicochemical structure and thermal degradation of biomass. Bioresour Technol 2013;146:254–260.

[18] Jensen P, Frandsen F, Dam-Johansen K, Sander B. Experimental investigation of the transformation and release to gas phase of potassium and chlorine during straw pyrolysis.

Energy & Fuels 2000;14:1280–1285.

[19] Nowakowski DJ, Jones JM, Brydson RMD, Ross AB. Potassium catalysis in the pyrolysis behaviour of short rotation willow coppice. Fuel 2007;86:2389–2402.

[20] Jones JM, Darvell LI, Bridgeman TG, Pourkashanian M, Williams A. An investigation of the thermal and catalytic behaviour of potassium in biomass combustion. Proc Combust Inst 2007;31 II:1955–1963.

[21] Raveendran K, Ganesh A, Khilar KC. Influence of mineral matter on biomass pyrolysis characteristics. Fuel 1995;74:1812–1822.

[22] Vassilev S V, Baxter D, Andersen LK, Vassileva CG, Morgan TJ. An overview of the organic and inorganic phase composition of biomass. Fuel 2012;94:1–33.

[23] Yang H, Yan R, Chen H, Lee DH, Zheng C. Characteristics of hemicellulose, cellulose and lignin pyrolysis. Fuel 2007;86:1781–1788.

[24] Eom IY, Kim KH, Kim JY, Lee SM, Yeo HM, Choi IG, Choi JW. Characterization of primary thermal degradation features of lignocellulosic biomass after removal of inorganic metals by diverse solvents. Bioresour Technol 2011;102:3437–3444.

[25] Werther J, Saenger M, Hartge EU, Ogada T, Siagi Z. Combustion of agricultural residues. Prog Energy Combust Sci 2000;26:1–27.

[26] Krigstin S, Wetzel S. A review of mechanisms responsible for changes to stored woody biomass fuels. Fuel 2016;175:75–86.

[27] Tillman DA. Biomass cofiring: The technology, the experience, the combustion consequences. Biomass and Bioenergy 2000;19:365–384.

[28] Vassilev S V., Vassileva CG, Vassilev VS. Advantages and disadvantages of composition and properties of biomass in comparison with coal: An overview. Fuel 2015;158:330–350.

[29] Boström D, Skoglund N, Grimm A, Boman C, öhman M, Broström M, Backman R. Ash transformation chemistry during combustion of biomass. Energy & Fuels 2012;26:85–93.

[30] Coelho P, Costa M. Combustão. 2a edition. Orion; 2012.

[31] Davis KA, Hurt RH, Yang NYC, Headley TJ. Evolution of char chemistry, crystallinity, and ultrafine structure during pulverized-coal combustion. Combust Flame 1995;100:31–40.

[32] Simões G. Single particle ignition of pulverized solid biomass fuels : experiments and modeling. MSc Thesis, Instituto Superior Técnico, 2016.

[33] Biagini E, Fantei A, Tognotti L. Effect of the heating rate on the devolatilization of biomass residues. Thermochim Acta 2008;472:55–63.

[34] Di Blasi C. Modeling chemical and physical processes of wood and biomass pyrolysis. Prog Energy Combust Sci 2008;34:47–90.

[35] Mani T, Murugan P, Abedi J, Mahinpey N. Pyrolysis of wheat straw in a thermogravimetric analyzer: Effect of particle size and heating rate on devolatilization and estimation of global kinetics. Chem Eng Res Des 2010;88:952–958.

[36] Lu H, Ip E, Scott J, Foster P, Vickers M, Baxter LL. Effects of particle shape and size on devolatilization of biomass particle. Fuel 2010;89:1156–1168.

[37] Simões G, Magalhães D, Rabaçal M, Costa M. Effect of gas temperature and oxygen

concentration on single particle ignition behaviour of biomass fuels. Proc Combust Inst 2016;0:1–8.

[38] Raveendran K, Ganesh A. Adsorption characteristics and pore-development of biomass-pyrolysis char. Fuel 1998;77:769–781.

[39] Di Blasi C. Combustion and gasification rates of lignocellulosic chars. Prog Energy Combust Sci 2009;35:121–140.

[40] Aarna I, Suuberg EM. Changes in reactive surface area and porosity during char oxidation. Symp Combust 1998;27:2933–2939.

[41] Mourant D, Wang Z, He M, Wang XS, Garcia-Perez M, Ling K, Li CZ. Mallee wood fast pyrolysis: Effects of alkali and alkaline earth metallic species on the yield and composition of bio-oil. Fuel 2011;90:2915–2922.

[42] Asadieraghi M, Wan Daud WMA. Characterization of lignocellulosic biomass thermal degradation and physiochemical structure: Effects of demineralization by diverse acid solutions. Energy Convers Manag 2014;82:71–82.

[43] Perander M, Demartini N, Brink A, Kramb J, Karlström O, Hemming J, Moilanen A, Konttinen J, Hupa M. Catalytic effect of Ca and K on CO2 gasification of spruce wood char. FUEL 2015;150:464–472.

[44] Fuentes ME, Nowakowski FJ, Kubacki ML, Cove JM, Bridgeman TG, Jones JM. Survey of influence of biomass mineral matter in thermochemical conversion of short rotation willow coppice. J Energy Inst 2008;81:234–241.

[45] Mayer ZA, Apfelbacher A, Hornung A. Effect of sample preparation on the thermal degradation of metal-added biomass. J Anal Appl Pyrolysis 2012;94:170–176.

[46] Jensen A, Dam-Johansen K, Wójtowicz M, Serio M. TG-FTIR Study of the Influence of Potassium Chloride on Wheat Straw Pyrolysis. Energy & Fuels 1998;12:929–938.

[47] Liu X, Bi XT. Removal of inorganic constituents from pine barks and switchgrass. Fuel Process Technol 2011;92:1273–1279.

[48] Eom IY, Kim JY, Kim TS, Lee SM, Choi D, Choi IG, Choi JW. Effect of essential inorganic metals on primary thermal degradation of lignocellulosic biomass. Bioresour Technol 2012;104:687–694.

[49] Werkelin J, Skrifvars BJ, Zevenhoven M, Holmbom B, Hupa M. Chemical forms of ash-forming elements in woody biomass fuels. Fuel 2010;89:481–493.

[50] van Lith SC, Jensen PA, Frandsen FJ, Glarborg P. Release to the gas phase of inorganic elements during wood combustion. Part 2: Influence of fuel composition. Energy and Fuels 2008;22:1598–1609.

[51] Johansen JM, Jakobsen JG, Frandsen FJ, Glarborg P. Release of K, Cl, and S during pyrolysis and combustion of high-chlorine biomass. Energy and Fuels 2011;25:4961–4971.

[52] Fahmi R, Bridgwater A V., Darvell LI, Jones JM, Yates N, Thain S, Donnison IS. The effect of alkali metals on combustion and pyrolysis of Lolium and Festuca grasses, switchgrass and willow. Fuel 2007;86:1560–1569.

[53] Kopyscinski J, Rahman M, Gupta R, Mims CA, Hill JM. K2CO3 catalyzed CO2 gasification of

ash-free coal. Interactions of the catalyst with carbon in N2 and CO2 atmosphere. Fuel 2014;117:1181–1189.

[54] Glarborg P. Hidden interactions-Trace species governing combustion and emissions. Proc Combust Inst 2007;31 I:77–98.

[55] Blomberg T. A thermodynamic study of the gaseous potassium chemistry in the convection sections of biomass fired boilers. Mater Corros 2011;62:635–641.

[56] Lawson-wood K, Robertson I. Study of the Decomposition of Calcium Oxalate Monohydrate using a Hyphenated Thermogravimetric Analyser - FT-IR System (TG-IR). PerkinElmer, Hyphenation, Application Note, 2016.

[57] Dollimore D. The thermal decomposition of oxalates. A review. Thermochim Acta 1987;117:331–363.

[58] Faúndez J, Arenillas A, Rubiera F, García X, Gordon AL, Pis JJ. Ignition behaviour of different rank coals in an entrained flow reactor. Fuel 2005;84:2172–2177.

[59] Riaza J, Khatami R, Levendis YA, Álvarez L, Gil M V., Pevida C, Rubiera F, Pis JJ. Combustion of single biomass particles in air and in oxy-fuel conditions. Biomass and Bioenergy 2014;64:162–174.

[60] Su S, Pohl JH, Holcombe D, Hart JA. Techniques to determine ignition, flame stability and burnout of blended coals in p. f. power station boilers. Prog Energy Combust Sci 2001;27:75–98.

[61] Zhang D, Wall TF. Ignition of coal particles : the influence of experimental technique. Fuel 1994;73:1114–1119.

[62] Yuan Y, Li S, Li G, Wu N, Yao Q. The transition of heterogeneous-homogeneous ignitions of dispersed coal particle streams. Combust Flame 2014;161:2458–2468.

[63] Howard JB, Essenhigh RH. The mechanism of ignition of pulverized coal. Combust Flame 1965;9:337–339.

[64] Howard JB, Essenhigh RH. Mechanism of solid-partical combustion with simultaneous gas-phase volatiles combustion. Symp Combust 1967;11:399–408.

[65] Wall TF, Phong-Anant D, Gururajan VS, Wibberley LJ, Tate A, Lucas J. Indicators of ignition for clouds of pulverized coal. Combust Flame 1988;72:111–118.

[66] Ruiz M, Annamalai K, Dahdah T. An Experimental Study on Group ignition of coal particle streams. Heat Mass Transf. Fires Combust. Syst., vol. 148, 1990, p. 19–26.

[67] Tomeczek J, Wójcik J. A method of direct measurement of solid fuel particle ignition temperature. Symp. Combust., 1991, p. 1163–1167.

[68] Molina A, Shaddix CR. Ignition and devolatilization of pulverized bituminous coal particles during oxygen/carbon dioxide coal combustion. Proc Combust Inst 2007;31 II:1905–1912.

[69] Shaddix CR, Molina A. Particle imaging of ignition and devolatilization of pulverized coal during oxy-fuel combustion. Proc Combust Inst 2009;32 II:2091–2098.

[70] Riaza J, Khatami R, Levendis YA, Álvarez L, Gil M V., Pevida C, Rubiera F, Pis JJ. Single particle ignition and combustion of anthracite, semi-anthracite and bituminous coals in air and simulated oxy-fuel conditions. Combust Flame 2014;161:1096–1108.

[71] Khatami R, Stivers C, Joshi K, Levendis YA, Sarofim AF. Combustion behaviour of single particles from three different coal ranks and from sugar cane bagasse in O2/N2 and O2/CO2 atmospheres. Combust Flame 2012;159:1253–1271.

[72] Bejarano PA, Levendis YA. Single-coal-particle combustion in O2/N2 and O2/CO2 environments. Combust Flame 2008;153:270–287.

[73] Khatami R, Stivers C, Levendis YA. Ignition characteristics of single coal particles from three different ranks in O2/N2 and O2/CO2 atmospheres. Combust Flame 2012;159:3554–3568.

[74] Levendis YA, Joshi K, Khatami R, Sarofim AF. Combustion behaviour in air of single particles from three different coal ranks and from sugarcane bagasse. Combust Flame 2011;158:452–465.

[75] Ferreira A. Caracterização Experimental da Ignição de Partículas Isoladas de Biomassa e Lenhite. MSc Thesis, Instituto Superior Técnico, 2016.

[76] Liu H, Zailani R, Gibbs BM. Comparisons of pulverized coal combustion in air and in mixtures of O 2/CO 2. Fuel 2005;84:833–840.

[77] Magalhães D. Ignition behaviour of single biomass and coal particles. MSc Thesis, Instituto Superior Técnico, 2015.

[78] Mason PE, Darvell LI, Jones JM, Pourkashanian M, Williams A. Single particle flame-combustion studies on solid biomass fuels. Fuel 2015;151:21–30.

[79] Ferreiro AI, Rabaçal M, Costa M. A combined genetic algorithm and least squares fitting procedure for the estimation of the kinetic parameters of the pyrolysis of agricultural residues. Energy Convers Manag 2016;125:290–300.

[80] Heitor M V., Moreira ALN. Probe Measurements of Scalar Properties in Reacting Flows. Combust. Flow Diagnostics, 1992, p. 79–136.

[81] Shaddix CR. Correcting thermocouple measurements for radiation loss: A critical review. 33rd Natl. Heat Transf. Conf., New York: American Society of Mechanical Engineers; 1999.

[82] Cleveland WS. Robust Locally Weighted Regression and Smoothing Scatterplots. J Am Stat Assoc 1979;74:829–836.

[83] Stenseng M, Jensen A, Dam-Johansen K. Investigation of biomass pyrolysis by thermogravimetric analysis and differential scanning calorimetry. J Anal Appl Pyrolysis 2001;58–59:765–780.